

1

Preparation of Artificial Metalloenzymes

Jared C. Lewis and Ken Ellis-Guardiola

Department of Chemistry, University of Chicago, 5735 S. Ellis Ave., Chicago, 60637, IL, USA

1.1 Introduction

Artificial metalloenzymes (ArMs) have the potential to merge key benefits of transition metal catalysts, particularly their ability to catalyze a wide range of challenging transformations, with those of enzymes, including their evolvability and capacity for molecular (i.e., substrate) recognition [1]. These topics and more are discussed in detail elsewhere in this volume, but their pursuit requires robust methods for ArM formation. Such methods are in and of themselves quite challenging to develop. Site-specific metal incorporation is required to ensure that single-site catalysts can be obtained. Compatibility with a wide range of metals and scaffolds is desirable to maximize the range of chemistries that can be explored. Compatibility with aqueous, ideally aerobic, reaction conditions and a wide range of functional groups, including those found in cellular milieu, are also important. An additional synthetic challenge is faced for ArMs generated from preformed catalysts, since these inherently reactive molecules must first be linked to scaffold anchoring moieties to generate ArM cofactors.

The hybrid nature of ArMs also complicates their characterization since distinct methods have conventionally been used for analysis of transition metal complexes and proteins. Various spectroscopies, including UV/Vis and electron paramagnetic resonance (EPR), can provide some insight into the metal primary coordination sphere [2], while dichroism spectrum (CD) and fluorescence spectroscopies can provide information on scaffold folding [3–5]. In some cases, NMR spectroscopy can also be used, but its utility is often limited by the high molecular weight of many scaffold proteins [6]. Inductively coupled plasma-mass spectrometry (ICP-MS) can be used to determine scaffold:metal stoichiometry, but not metal location within the scaffold [6]. High resolution MALDI and ESI MS can also be used to determine extent of cofactor incorporation and scaffold modification in general [4]. Of course, X-ray crystallography remains the best option for unambiguously charactering metal location and coordination environment within ArMs, but this technique is often complicated by conformational flexibility and variable occupancy of introduced metal centers [7].

Despite these challenges, a large number of methods have been developed that possess some or all of the properties noted above. The aim of this chapter is to provide an overview of key methodology developments. These will be broken into sections in which scaffold metalation is governed predominately by metal binding by scaffold residues (Section 1.2), non-covalent cofactor binding either to the catalyst itself or to a catalyst substituent (Section 1.3) and, finally, covalent scaffold modification using functionalized cofactors (Section 1.4). ArM formation often involves elements of multiple methods (e.g., ligation of a metal in a covalently linked cofactor or metalation of ligands that are introduced via a non-covalent scaffold binding), but this classification helps to address many unique features, advantages, and disadvantages of different methods of ArM formation.

1.2 ArM Formation via Metal Binding

A wide range of homogeneous metal catalysts can be prepared by combining appropriate quantities of a metal catalyst precursor (M) with one or more small molecule ligands (L) [8]. Several of the 20 canonical amino acids possess residues capable of binding to a wide range of transition metals via N, O, or S coordination. Protein scaffolds can organize these residues into well-defined three-dimensional chiral arrays metal binding sites. The reactivity conferred to metal centers by these binding sites has led to the evolution of metalloenzymes that catalyze a range of challenging organic transformations in nature [9], including nondirected C—H bond functionalization [10]. Inspired by the synthetic power of these natural metalloenzymes, researchers have explored the use of protein scaffolds as ligands for nonnative metal ions to generate ArMs that catalyze a variety of organic transformations (Figure 1.1) [11].

1.2.1 Repurposing Natural Metalloenzymes

Given their inherent metal-binding capabilities, natural metalloenzymes have obvious potential as scaffolds for ArM formation. In addition to metal binding, many metalloenzymes have active sites that evolved to bind small molecule substrates, providing additional space for unnatural substrates to bind. Of course, conditions must first be developed to extract native metal ions from a metalloenzyme of interest and to incorporate the desired metal ion or fragment

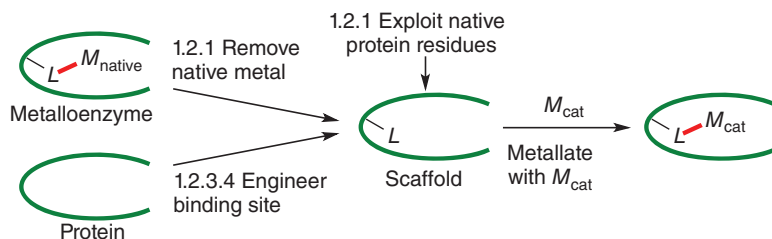


Figure 1.1 Approaches to generate ArMs via metal binding.

without denaturing the scaffold. Once this is accomplished, however, it is often possible to incorporate a range of metal ions into the scaffold, and established methods for characterization of the native metalloenzyme can often be applied to the resulting ArM.

1.2.1.1 Carboxypeptidase A

Emil Kaiser's research group at the University of Chicago was one of the first to leverage the metal binding site of a natural metalloenzyme to form ArMs with novel reactivity. Carboxypeptidase A (CPA), a Zn(II)-containing metalloenzyme containing a His/His/Glu binding site, was dialyzed against 1,10-phenanthroline to generate the apoenzyme, which was subsequently metalated with a variety of metal(II) salts. The Cu(II)-CPA construct was found to catalyze the oxidation of ascorbic acid and to exhibit Michaelis–Menten kinetics, mimicking the activity of other Cu(II)-containing redox enzymes [12]. While this work established the potential for a metal binding site to be employed for nonnative metal binding and catalysis, unspecified spectroscopic characterization was reported to indicate significant perturbation of the coordination environment around the metal. This alteration was later confirmed by crystallographic studies using Hg(II)-CPA, which highlighted the importance of characterizing the primary coordination sphere of metal fragments incorporated into protein scaffolds [13].

1.2.1.2 Carbonic Anhydrase

Carbonic anhydrases (CAs), also Zn(II)-containing metalloenzymes but containing His₃ binding sites, have subsequently been utilized for ArM formation by a number of researchers. As in the case of CPA, zinc(II) can be removed from CAs by dialysis against a chelating agent (1,10 phenanthroline or 2,6-pyridinedicarboxylate) to afford the apoproteins [14]. Incubation of the apoprotein with metal(II) salts results in metal-substituted CAs. These nonnative constructs were initially explored for their interesting spectroscopic and structural properties, including significantly distorted coordination geometries [15, 16]. Kazlauskas and Soumillion later demonstrated that substitution of bovine carbonic anhydrase (bCA) isoforms I and II and human carbonic anhydrase isoform II (hCAII) with manganese(II) afforded redox-active variants of the enzyme that exhibited peroxidase-like activity [14, 17]. Incubating apo-CA with substoichiometric quantities of Mn(OAc)₂ or excess MnCl₂ followed by dialysis against buffer provided ArMs free of free metal salts. Mn(II) loading was confirmed by loss of native CA activity and quantitated by ICP-AES. Alkene epoxidations catalyzed by these ArMs proceeded with generally low to moderate yields and enantioselectivities.

One of the challenges to preparing ArMs via metal substitution of apo-metalloenzymes is the possibility for nonspecific binding of metals to non-active site residues. For example, metalation of apo-hCA(II) with [Rh(cod)₂]BF₄ led to extensive nonspecific binding, with 6–8 rhodium ions bound to the protein monomer as determined by ICP-MS [18]. Unlike Mn(II) salts, which show low epoxidation activity relative to the corresponding CA ArMs, [Rh(cod)₂]BF₄ can efficiently catalyze the target reaction, enabling a non-selective reaction pathway that can compete to the detriment of the overall

stereoselectivity of the transformation. To address this issue, Kazlauskas used mutagenesis to remove from hCAII several surface histidine residues that were hypothesized to be sites of nonspecific Rh binding. Mutating these histidine residues to arginine, phenylalanine, or alanine provided 9^* His-hCAII-[Rh], which bound significantly fewer Rh ions (an average of 1.8 Rh/hCAII) and provided improved selectivity for hydrogenation of *cis*-stilbene relative to competing isomerization of this substrate to *trans*-stilbene. Kazlauskas later demonstrated that metalation of 9^* His-hCAII with $[\text{Rh}(\text{CO})_2(\text{acac})]$ reduces the Rh/hCAII ratio to 1.2. The resulting ArM catalyzed styrene hydroformylation with improved selectivity for the linear aldehyde over free $[\text{Rh}(\text{CO})_2(\text{acac})]$ or wild-type hCAII-[Rh], indicating that surface-bound rhodium preferentially yields the branched aldehyde and negatively impacts the selectivity of the hybrid [19].

A more recent study provided additional insights into the preparation and characterization of Rh-substituted CAs [6]. Evaluating apo-hCAII metalation by a panel of Rh complexes revealed that the extent of nonspecific surface binding by the metal is determined not only by the presence of coordinating residues outside of the active site but also by the identity of the ancillary ligands on the Rh complex. Extent of metalation was confirmed by competitive metalation with Co(II), which, when bound to hCAII, is known to catalyze the hydrolysis of 4-nitrophenyl acetate, enabling rapid spectrophotometric evaluation of activity. Using this method, the authors determined that Rh precursors with tighter binding ligands provided more reliable metalation at the active site, with $[\text{Rh}(\text{nbd})_2]\text{BF}_4$ and $\text{Rh}(\text{acac})(\text{CO})_2$ serving as particularly effective (>90% yield). NMR spectroscopy, previously used to study metal coordination in CA [20], also indicated that only two of the three His residues in the hCAII active site were coordinated to Rh, again showing that novel coordination modes can be achieved using native metal binding sites. Unique perturbations were also observed in the crystal structures of hCAII substituted with Co(II), Cu(II), Ni(II), and Mn(II), although in these cases His₃ binding was observed (Figure 1.2).

1.2.1.3 Metallo- β -lactamase

Recently, Itoh reported that the active site of a di-zinc metallo- β -lactamase from *Stenotrophomonas maltophilia* could be repurposed for copper binding [21]. Expression of the metalloenzyme in a medium containing a large excess of $\text{Cu}(\text{SO}_4)$ resulted in the formation of a dinuclear copper enzyme similar to type III copper proteins, which catalyze the oxidation of phenols to catechols. Formation of a dinuclear copper enzyme with 1.7 Cu atoms per scaffold was confirmed by ICP-MS. An Asp residue in the His/His/Asp binding site of the metallo- β -lactamase was mutated to His to match the two His/His/His motifs in type III copper proteins. This yielded an ArM catechol oxidase that oxidized 4-*tert*-butyl-catechol with 36-fold greater efficiency than the di-zinc metallo- β -lactamase. It should be noted that the His/His/His binding site was optimized not only by introducing a proximal histidine but also by increasing the conformational flexibility of a histidine through the mutation of a histidine-adjacent proline to glycine [21].

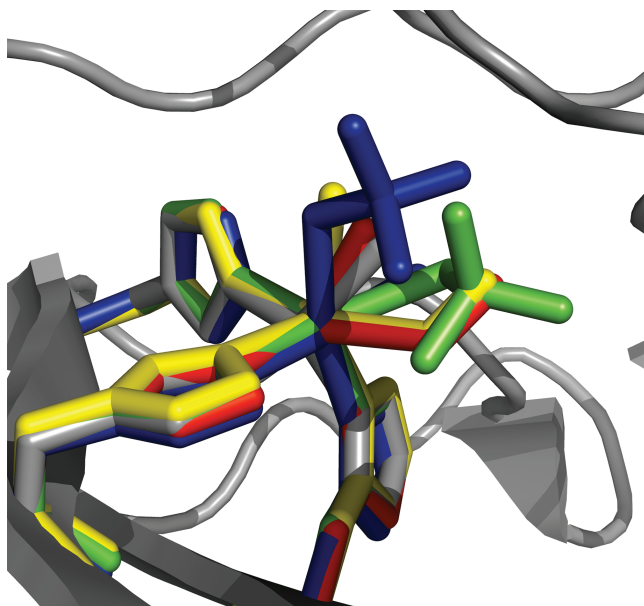


Figure 1.2 Overlay of His/His/His metal binding site in hCAII structures containing Zn(II) (gray), Co(II) (red), Cu(II) (yellow), Ni(II) (blue), and Mn(II) (green) bearing $\text{H}_2\text{O}/\text{O}_2$ (Zn, Cu, and Co) and sulfate (Ni and Mn) ligands.

1.2.1.4 Ferritin

CPA and hCA illustrate the potential of metalloenzymes as scaffolds for ArM formation via metal binding. These small monomeric enzymes, however, represent only a small fraction of the types of metal-binding proteins that could be used for ArM formation. For example, self-assembled multimeric protein scaffolds have the potential to control cofactor reactivity at both nano- and mesoscales. This approach has been most extensively explored using ferritin, an iron storage protein comprised of 24 subunits that assemble into a cage-like sphere with an ~ 8 nm internal diameter [22] capable of accommodating of up to 4500 Fe ions [23]. Robust procedures to demineralize ferritins via dialysis against thioglycolic acid can be used to generate apoferritin for ArM formation [22].

Watanabe first reported that apo-recombinant light chain horse liver ferritin (rHLFr) (Figure 1.3a) could be loaded with 96 equiv. of the [Pd(allyl)] fragment based on ICP-MS analysis following incubation with $[\text{Pd}(\text{allyl})\text{Cl}]_2$. The resulting ArM catalyzed the Suzuki coupling of phenylboronic acid with 4-iodoaniline [23], and the ArM crystal structure revealed two unique binding sites for dinuclear [Pd(allyl)] adducts on each subunit for a total of four Pd atoms per subunit (Figure 1.3b and c, top). Pd binding and stoichiometry could be altered via site-directed mutagenesis [24, 25], but this had little impact on the overall catalytic efficiency of the ArM [23]. In a similar manner, $[\text{Rh}(\text{nbd})\text{Cl}]_2$ was introduced into the apo-rHLFr scaffold, leading to 72 bound rhodium centers in three unique binding sites per subunit (Figure 1.3b and c, bottom) as determined by crystallography and ICP-OES (inductively coupled plasma-optical

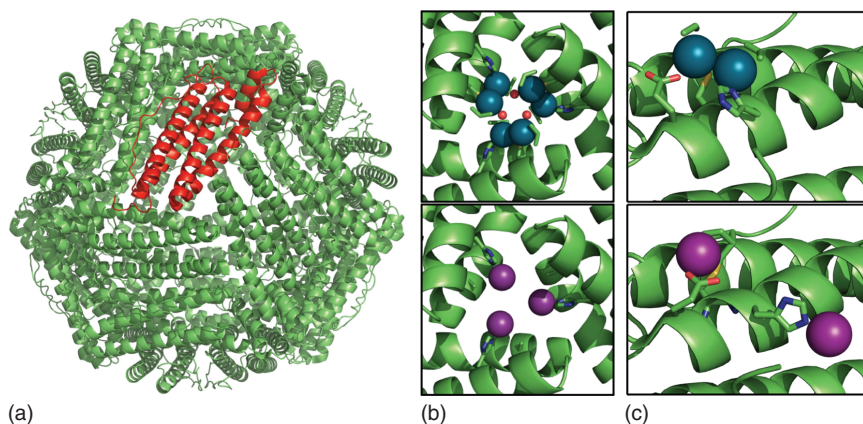


Figure 1.3 (a) Apo-recombinant horse liver ferritin with highlighted subunit in red. (b) Ferritin threefold axis binding site occupied with Pd(II) (top, blue spheres) and Rh(I) (bottom, purple spheres). (c) Ferritin accumulation binding site with Pd(II) (top, blue spheres) and Rh(I) (bottom, purple spheres).

emission spectrometry) [22]. In one of these binding sites, migratory insertion of a Rh-bound cysteine residue into a norbornadiene ligand resulted in a covalent cysteine–norbornadiene linkage. This ArM catalyzed phenylacetylene polymerization, giving rise to polyphenylacetylene that remained solubilized within the ferritin scaffold. The solubility of the polymer was determined to arise because of association of the polymer with ferritin, which was corroborated by co-elution of the polymer and ferritin during size exclusion chromatography. In contrast, the small-molecule catalyzed reaction gave the insoluble polymer. In addition, the ArM produced a molecular weight-restricted set of polymer products with a narrow polydispersity relative to $[\text{Rh}(\text{nbd})\text{Cl}]_2$ under the same conditions, indicating that the ferritin plays a critical role in defining and altering the polymerization environment [26]. Finally, both the ruthenium complex $[\text{Ru}(p\text{-cymene})\text{Cl}_2]_2$ and the iridium complex $[\text{IrCp}^*\text{Cl}_2]_2$ have been introduced into the apoferritin scaffold, and while binding of the metals has been corroborated by crystallography and ICP-OES, no catalysis by these constructs has been reported [27, 28].

1.2.2 Exploiting Serendipitous Metal Binding by Proteins

While nonnative metal coordination by apo-metalloenzymes offers an attractively simple approach for ArM formation, it is limited to coordination motifs present in natural metalloenzymes. Given that over half of the canonical amino acids possess side chains that can coordinate to metals, however, it is not surprising that many proteins, not just metalloenzymes, can bind to metal ions. Indeed, serendipitous metal binding was noted above as a potential complication for selective metalation of apo-metalloenzymes, but if selective, it provides a means to significantly expand the range of ArMs that can be generated via metal binding. Operationally, this is one of the simplest methods for ArM formation; any soluble, isolable protein can be explored for metal binding and

catalytic competence. Because the metal-binding site in these scaffolds is not known, however, characterizing the resulting ArMs and subsequent rational modification can be challenging. Furthermore, the absence of any defined substrate binding site means that fortuitous interactions are also required to impart selectivity to reactions that occur at the metal center.

Serum albumins have been extensively examined as ArM scaffolds. These proteins mediate the transport and distribution of numerous species present in blood serum, including organic molecules and inorganic cations of zinc, calcium, and copper [29]. The stability and low cost of serum albumins has led to their use for numerous synthetic applications [30] and metal coordination [31]. Building on this precedent, Marchetti established that an ArM formed from human serum albumin (HSA) and $\text{Rh}(\text{CO})_2(\text{acac})$ catalyzed olefin hydroformylation [32]. The scaffold flexibility enabled by serendipitous metal binding was illustrated by subsequent metalation of bovine serum albumin (BSA), egg albumin, and papain, three commercially available proteins, with $\text{Rh}(\text{CO})_2(\text{acac})$ to generate ArM hydroformylases with different selectivity relative to that of Rh–HSA [32]. The HSA–Rh ArM also catalyzed hydrogenation of α,β -unsaturated aldehydes and ketones with high chemoselectivity for olefin reduction (relative to other albumins), but no enantioselectivity toward prochiral substrates [33]. This result is consistent with MALDI-MS data, showing that this ArM possesses several Rh centers [34].

Serum albumins have also been found to bind high-valent transition metal oxo complexes to form ArMs that catalyze various oxidative transformations. Kokubo first reported that a 1 : 1 mixture of BSA and OsO_4 generated an active alkene dihydroxylation catalyst [35]. Comparison of the UV/Vis spectrum of the single-turnover product of α -methylstyrene dihydroxylation with a corresponding small molecule analogue (with an ethylenediamine backbone) suggested that OsO_4 was likely bound to BSA via two primary amines, implicating lysine residues as ligands [35].

More recently, Ward found that OsO_4 was bound to streptavidin and that the resulting ArM catalyzed dihydroxylation of various alkenes [36]. Scaffold mutagenesis led to altered enantioselectivity, suggesting that the active catalyst is bound within the protein scaffold, but anomalous X-ray diffraction revealed multiple OsO_4 binding sites [36]. Ward also explored the incorporation of $[\text{VO}]^{2+}$ into streptavidin and showed that the resulting ArM catalyzed enantioselective sulfoxidation of aryl thioethers [37]. The vanadyl ion was bound to the biotin-binding site of streptavidin as evidenced by the loss of enantioselectivity in the presence of biotin. Interestingly, Asp-128, which is important for biotin binding, is also involved in vanadium binding, likely via hydrogen bonding interactions, since obvious perturbation in ligand field was not observed upon metal binding by EPR spectroscopy. Importantly, rate enhancement over free $[\text{VO}]^{2+}$ was observed [37], and similar scaffold acceleration has become increasingly common in ArM catalysis [38].

Vanadium-containing ArMs have previously been explored by Sheldon. Based on structural similarities between phytase and vanadium chloroperoxidase, it was hypothesized that introducing vanadate into phytase scaffolds could generate an ArM chloroperoxidase. Indeed, treating *Aspergillus ficuum*

phytase with vanadate inhibited phytase-catalyzed hydrolysis of *p*-nitrophenyl phosphate, presumably via binding in the oxyanion hole in the phytase active site [39]. The resulting phytase–vanadate ArMs also catalyzed sulfoxidation of sulfides with modest enantioselectivity mimicking the reactivity of vanadium chloroperoxidase [40]. Rate enhancement over free vanadate was again observed. Importantly, the peroxidase activity of other scaffolds (albumin, other phytases, acid phosphatase, phospholipase D, aminoacylase, sulfatase) was readily evaluated. The resulting ArMs also possessed sulfoxidase activity, albeit with lower efficiency and enantioselectivity than that of the *A. ficuum* phytase/ VO_4^{3-} system [41].

Ueno has also explored the possibility of exploiting the supramolecular architectures formed by protein crystals for heterogeneous ArM catalysis. Hen egg white lysozyme (HEWL) can be crystallized into two forms: O (orthorhombic) and T (tetragonal). The T form has been shown to bind $[(\eta^6\text{-}p\text{-cymene})\text{-RuCl}_2(\text{H}_2\text{O})]$ complexes that can be introduced into the protein crystals by soaking [42]. More recently HEWL crystals of both O and T forms were prepared and cross-linked with glutaraldehyde to enhance crystal stability, and $[\text{Ru}(\text{benzene})\text{Cl}_2]_2$ was then introduced by soaking. Crystallographic studies revealed that the metal complex bound to discrete, solvent-channel exposed positions on the HEWL monomers and the binding stoichiometry observed was corroborated by ICP-OES. These ArM-catalyzed reductions of a variety of acetophenone derivatives with modest conversions and enantioselectivities and cross-linked crystalline catalyst could be recycled 10 times (albeit with ~70% decrease in conversion and enantioselectivity) [41].

1.2.3 Designing Metal-Binding Sites in Scaffold Proteins

The examples presented in the previous two sections highlight strategies by which nonnative metals have been introduced into naturally occurring metal binding sites to generate ArMs. Significant effort has also been devoted to designing metal binding sites into proteins and designing metal binding proteins *de novo*. These approaches have the potential to significantly expand the range of coordination geometries and scaffolds that can be used for ArM formation via metal binding. Of course potential scaffolds must not only favor metal binding in the designed binding site over other possible binding sites as discussed above but also accommodate the designed metal-binding site to begin with. Impressive progress toward the design of metal binding proteins has been made, and many examples of ArM formation via this approach have been reported.

A straightforward example of this approach was accomplished by Reetz and coworkers, who introduced a Cu(II)-binding His/His/Asp triad within the TIM-barrel protein tHisF based on inspection of the protein crystal structure (Figure 1.4a). The resulting ArM catalyzed the Diels–Alder reaction of aza-chalcones with modest enantioselectivity, illustrating how otherwise “vacant space” within a scaffold can be used to generate an ArM active site [43]. In a strategy echoing that was seen with CA, potential competing metal binding sites were systematically eliminated to enhance the selectivity of the target reaction, and selective metal incorporation was supported by EPR spectroscopy [44].

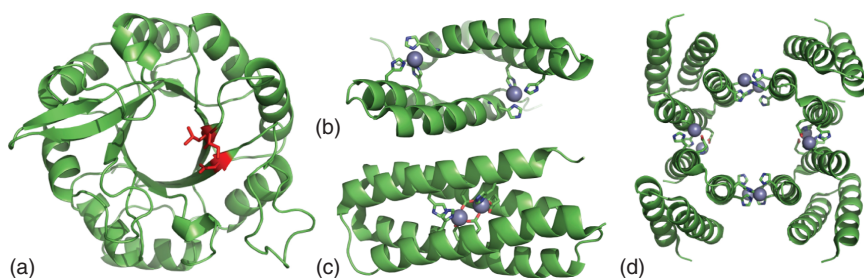


Figure 1.4 Locations of metal binding sites introduced into scaffold proteins. (a) tHisF scaffold with mutation sites in red. (b) Rab4 Zn-directed homodimer crystal structure with Zn(II) represented with gray spheres. (c) NMR structure of 3His-G4DFsc bound to two Zn(II) ions (gray spheres). (d) Crystal structure of Zn₈-^{A104/G57}AB34 with structural Zn(II) sites on the vertical axis and catalytic Zn(II) sites on the horizontal axis.

Metal binding sites have also been designed at protein–protein interfaces to create ArMs. For example, Zn-binding sites were introduced into the Rab4 binding domain of rabenosyn to generate Zn-directed homodimers (Figure 1.4b) [45]. Notably, according to crystal structure of the dimer, Zn was coordinated by three histidine residues rather than the expected four. The fourth coordination site was occupied by the carboxylate oxygen of tartrate, leading to a His₃–carboxylate ligand environment reminiscent of many Zn-dependent metalloenzymes. Indeed, the resulting ArM catalyzed hydrolysis of *p*-nitrophenyl acetate.

In a similar effort, Tezcan employed the protein cytochrome *cb*₅₆₂ as a building block for creating Zn-directed self-assembling tetramers. The interface between monomers was used as a potential space for designing a catalytic zinc site. Based on the crystal structure of the tetramer, multiple designs for zinc coordination sites were prepared and interrogated for esterase activity. In a departure from previous examples, the strongest esterase activity arose from coordination by a Glu/His/His triad, which was confirmed by X-ray crystallography (Figure 1.4d). Remarkably, the resulting tetrameric assembly gives rise to *in vivo* ampicillin hydrolysis. This was exploited to perform a selection-based saturation mutagenesis study for the optimization of ampicillin hydrolysis. This ultimately yielded a tetramer that gave a threefold enhanced hydrolysis activity. As such, it is the only example in which an ArM has been optimized using a survival-based selection and a rare example in which an ArM has shown catalytic activity *in vivo*.

The ArMs described thus far utilize proteins as scaffolds for metal-binding residues. In some cases involving enzyme scaffolds, ArM formation led to a loss of native activity, which, while providing a means to evaluate ArM formation [6, 14, 39], also suggested that the native function of scaffold proteins can be exploited for ArM function. Several early examples of such scaffold exaptation were illustrated by Lu, who developed functional models of heme–copper oxidase (HCO) by introducing two nonnative histidine residues (L29H and F43H) proximal to the heme–iron center in sperm whale myoglobin [2]. The His residues, in addition to the native His-64, formed a His/His/His copper-binding motif, as in HCO. This system was determined to be a competent, albeit inefficient,

heme oxygenase (HO) [46]. In a later study, a tyrosine residue was introduced to mimic a conserved tyrosine in HCO. The resultant ArM catalyzed reduction of O_2 to H_2O with >1000 TON (turnover number), clearly showing how tuning residues in the primary and secondary metal coordination spheres can improve ArM activity [47, 48].

Much of the work outlined above relied on inspection of X-ray structures to identify sites for installing metal-binding residues. In recent years, more studies have leveraged the capabilities of computational methods for identifying and designing metal binding sites in proteins. Programs like RosettaMatch [49] and RosettaDesign [50] have proven to be quite effective toward the design of metal binding sites [51]. Other tools, including search for three-dimensional atom motifs in protein structure (STAMPS) [52, 53], Urantein [54], and SUNS [55], have been developed to identify viable three-dimensional motifs [55]. Predicting catalytically competent metal binding sites remains a significant challenge for computational design methods. Efforts toward catalysis thus far have generally relied on the tandem approach of computational design to generate a panel of candidates that is then evaluated for catalytic function. For example, Ward recently used STAMPS to identify a number of candidate scaffolds with facial triad motifs. Screening these scaffolds with a panel of metal salts and oxidation conditions led to the identification of the N131D mutant of 6-phosphogluconolactonase, which, in the presence of $CuSO_4$ and hydrogen peroxide, yielded a competent ArM peroxidase. Metal binding was characterized by tryptophan-fluorescence quenching, crystallography, and EPR, revealing multiple Cu binding sites. The expected metal binding site showed the highest occupancy; the Cu was found to be coordinated by only two histidines, rather than a predicted facial triad. Mutagenesis studies revealed that this was indeed the site of catalysis. Overall, this strategy demonstrates the importance of predictive computational tools to enhance the likelihood of “serendipitous” metal binding [56].

Fundamental studies on the *de novo* design of proteins have led to many examples in which α -helical bundles can be used to template and manipulate metal binding sites. While the majority of these examples rely on self-assembly of synthetic short peptides, and therefore fall outside the scope of this chapter, a few notable examples of ArMs have emerged from this field. For example, Degrado and coworkers were able to express a *de novo* designed single chain *due ferri* (DFsc) *N*-oxidase. AurF, a *p*-aminobenzoate *N*-oxidase, is one of the few known *N*-oxidases in nature [57]. *In silico* design was employed to achieve optimal similarity between the diiron active sites of AurF and DFsc, the single-chain asymmetric analogue to the multimeric *de novo* designed DF enzyme [58, 59]. This required multiple second- and third-shell modifications to generate an ArM that could fold properly and bind the iron ions that constitute its dinuclear core. In addition, four glycine mutations were introduced in the active site channel to optimize substrate entry into the cavity. Characterization of M(II) (M=Fe or Co) binding and stoichiometry was carried out by NIR CD and UV/Vis titration studies, while the structure of the Zn(II)-substituted protein was confirmed by NMR (Figure 1.4c). The final engineered construct, 3His-G4DFsc, displayed AurF-like *N*-oxidase activity, leading to the *N*-hydroxylation of *p*-aminoanisole

(followed by decomposition to the corresponding nitroso compound). DFsc was also engineered to catalyze the two-electron oxidation of *p*-aminophenol [58], and, in a more recent effort, a structurally similar di-zinc ArM was engineered to stabilize a semiquinone radical, laying the groundwork to use similar reactive intermediates in ArM catalysis [60]. Together, these examples demonstrate the versatility of *in silico* design not only to improve the binding of metal ions but also to optimize the primary and secondary coordination spheres to tune catalytic activity and substrate access.

Pecoraro has recently demonstrated the use of a heterologously expressed single-chain three-helix bundle that displays CA activity. Using the *de novo* protein α 3D as a starting point, the group incorporated a Zn(II) site by mutating three leucine residues to histidine residues and removing a competing native histidine. The designed His/His/His coordinating motif enabled binding of Zn(II) with 50–190 nM affinity (determined by colorimetric zincon assay), and extended X-ray absorption fine structure (EXAFS) confirmed a tetrahedral (N/N/N/O) coordination geometry similar to that seen in CA. The resulting ArM catalyzed the hydration of CO₂ with efficiencies one to three orders of magnitude of those of CAs I–III [61]. This is slightly lower than a related multimeric homologue from the same group [62].

1.2.4 Introducing Metal-Binding Sites Using Unnatural Amino Acids

ArM formation via metal binding to protein scaffolds has traditionally been limited to the coordinating functionality offered by the 20 canonical amino acids. A far greater diversity of ligands, most of which have not been identified in nature, can be prepared in the laboratory to support small-molecule transition metal complexes. Researchers have long appreciated the potential for unnatural metal-binding residues to expand the range of metal binding sites that can be incorporated into proteins [63, 64]. Fortunately, advances in methodology for incorporating unnatural amino acids into proteins have enabled efforts to accomplish this goal [65].

Early studies by Lu investigated the role of the axial ligand in the copper-dependent electron transfer protein azurin. Expressed protein ligation [66] was used to replace the native axial ligand, Met121, with a host of unnatural amino acids (**1**, Figure 1.5) to investigate their effect on the reduction potential of the active site copper [67, 68]. The development of codon suppression methods for genetically encoding unnatural amino acids into proteins has rendered the incorporation process accessible to essentially any laboratory with standard cell culture capabilities [69]. On the other hand, engineering the tRNA/tRNA synthetase (aaRS) pairs required by these methods remains a more challenging endeavor.

Schultz reported the first example in which a metal-binding amino acid, bipyridyl alanine (BpyAla, **2**, Figure 1.5), was genetically encoded into a protein [70]. Identifying a suitable aaRS for BpyAla required a substrate walking approach in which an aaRS selective for biphenylalanine incorporation was used as an intermediate to identify a variant with the desired selectivity toward BpyAla. The resulting tRNA/aaRS pair was used to genetically encode a BpyAla

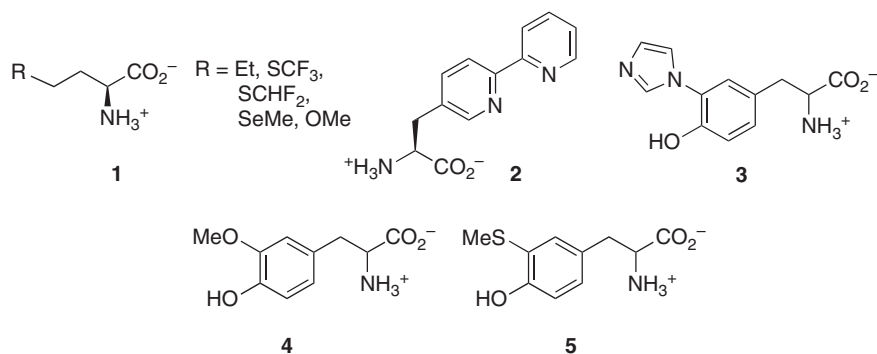


Figure 1.5 Structures of unnatural amino acids incorporated into protein scaffolds to create ArMs or improve ArM activity.

residue on the surface of bacteriophage T4 lysozyme in response to an amber codon. The resultant protein folded correctly, and incorporation of BpyAla was confirmed by electrospray ionization mass spectrometry (ESI-MS). Furthermore, in the presence of CuCl_2 , the BpyAla-containing scaffold showed a mass adduct corresponding to metalation, whereas the control containing tyrosine in the same position showed no metalation, suggesting that metalation occurs selectively at BpyAla.

As will be discussed later, bipyridyl complexes of Fe(II) and Cu(II) were used in some of the first ArMs generated using covalent bioconjugation methods. In analogy to these early studies, incorporation of BpyAla proximal to the DNA binding site of catabolite activator protein (CAP), followed by metalation of the resulting protein with Fe(II) and Cu(II), provided ArM nucleases [71]. The binding affinity of the CAP scaffold was not significantly perturbed, and the site-specific DNA cleavage was observed in the presence of air and a reducing agent (ascorbate or 3-mercaptopropionic acid). Similarly recapitulating earlier work on covalent ArMs (*vide infra*) [72], Roelfes demonstrated that introducing BpyAla into the dimer interface of Lactococcal multidrug resistance regulator (LmrR) followed by metalation with Cu(II) generated ArMs that catalyzed Friedel–Crafts alkylation with high enantioselectivity [73]. The incorporation of BpyAla into LmrR was confirmed by ESI-MS, and metalation of the bipyridyl side chain was characterized both by UV/Vis and Raman spectroscopy.

Baker recently demonstrated that RosettaMatch could be used to computationally design a high affinity metalloprotein containing BpyAla [51]. Initial designs yielded a protein that bound a series of divalent cationic transition metals, but a crystal structure of one of the metalated structures revealed that the coordination of iron by the protein-bound BpyAla was joined with binding of two other bpy monomers (free in solution) to form the highly stable octahedral tris(bpy) complex outside of the intended active site. A second round of design incorporating metal coordination by other scaffold residues and water molecules to support an octahedral geometry at various M(II) centers ($M = \text{Co}, \text{Zn}, \text{Fe}, \text{Ni}$) within the chosen scaffold was then pursued. Ultimately, of the 28 designed systems, only 9 expressed as soluble proteins, and 8 of these bound metals in a BpyAla-dependent

manner (determined by UV/Vis spectroscopy) without the spectroscopic signature of the octahedral tris(Bpy) complex [51].

Genetic incorporation of various tyrosine derivatives has been used to improve the activity of the HCO ArMs noted above [47, 48]. For example, imidazole-substituted tyrosine derivative (3) [74] and 3-methoxytyrosine (4) [75] were introduced into the cytochrome *c* oxidase (CcO) mimic Cu_bMb [48], yielding a series of ArMs with significantly improved oxidase activity over Cu_bMb and Y33- Cu_bMb . Unnatural amino acid incorporation was validated by ESI-MS of the resulting ArMs. The lower reduction potential of the 3-methoxytyrosine was implicated in the increased ArM oxidase activity, as it is known that both lowered $\text{p}K_a$ and reduction potential improve the designed enzyme's ability to fully reduce oxygen to water. In a similar effort, a cytochrome *c* nitrite reductase mimic based on the native myoglobin scaffold was modified with 3-methylthiotyrosine (5) at position 33, enhancing its activity toward hydroxylamine reduction fourfold relative to the simple tyrosine derivative [76].

1.3 ArM Formation via Supramolecular Interactions

As previously noted, the potential to tune metal reactivity using small molecule ligands is one of the great strengths of homogeneous transition metal catalysis. The great diversity of synthetic small molecule ligands gives chemists extensive control over catalyst activity and selectivity [8]. As noted above, codon suppression methods can be used to introduce non-proteinogenic metal-binding amino acids into proteins, but only a few examples have been reported for ArM formation, and the process of engineering biosynthetic machinery for this purpose remains challenging. In nature, posttranslational modifications can lead to metal binding motifs, but this is still limited in terms of the range of ligands that can be generated [77].

To expand the scope of metal binding motifs in protein scaffolds and thus reaction scope of ArMs, researchers have explored incorporation of synthetic cofactors (metal complexes or non-proteinogenic ligands that can be subsequently metalated). This has been accomplished using both supramolecular interactions and covalent linkages, which are covered in this and the following section. The supramolecular methods explored to date can be further divided into two categories: cofactor binding or cofactor anchoring (Figure 1.6). In the former, metal cofactors are bound directly by a scaffold protein, while in the

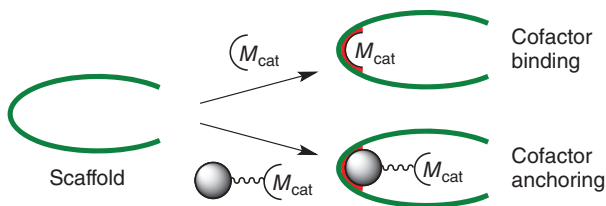


Figure 1.6 ArM formation via cofactor binding and cofactor anchoring.

latter, catalysts are tethered to an anchoring group that is bound by the scaffold protein. In both cases, additional binding interactions between the cofactor metal center and scaffold residues can occur. The cofactor reactivity is thus largely defined by the catalyst structure, and the protein scaffold provides a means to modulate this reactivity and to control selectivity.

1.3.1 Cofactor Binding

Just as native and serendipitous metal ion binding by protein scaffolds can be exploited for ArM formation, so too can native and serendipitous cofactor binding. Relatively simple cofactors analogous to those that might be used for small molecule catalysis (i.e., lacking anchoring groups) can often be incorporated into proteins. Cofactor binding is typically confirmed and quantitated using mass spectrometry or spectroscopic methods used to characterize the cofactor itself. Because active catalysts are often used as cofactors, high binding affinity is essential to ensure that nonselective background reactions do not dominate catalysis. Unlike metal binding, however, cofactor binding involves supramolecular interactions that are often not conserved with even minor changes in cofactor structure, leading to potential variability between ArM active sites involving similar cofactors [78]. Because of this, additional characterization is required to determine the location of the cofactor within the ArM. In some cases, direct metal binding by scaffold residues can be monitored spectroscopically, and mutagenesis can be used to determine scaffold residues that perturb spectroscopic observables related to metal binding. Ultimately, X-ray crystallography must often be used to provide definitive information regarding cofactor placement within ArMs.

1.3.1.1 Heme Proteins

The apo-forms of heme proteins were among the first scaffolds used for ArM formation via cofactor binding. Myoglobin in particular has been extensively studied in this regard and has provided a number of insights into synthetic cofactor incorporation into protein scaffolds. Apo-myoglobin has most frequently been prepared via heme extraction using organic solvents under acidic conditions [79]. More recently, Watanabe reported conditions for expressing apo-heme proteins, including myoglobin, that allowed for cofactor incorporation during cell lysis [79], and methods for direct expression of heme proteins with different cofactors have also been reported [80, 81]. Early studies by Watanabe established that nonnative peroxidase activity could be conferred to myoglobin via mutagenesis [82, 83]. Subsequent efforts demonstrated that apo-myoglobin reconstituted with nonnative Fe-porphyrin cofactors could be used to generate ArM peroxidases with altered substrate specificity and reactivity relative to the myoglobin mutants [84].

Myoglobin was also found to bind a number of synthetic metal complexes with relatively planar, often aromatic ligands in a similar manner to the native heme cofactor. For example, reconstitution with Mn(III) and Cr(III)–salophen cofactors (7; Figure 1.7) was used to generate ArM sulfoxidases with low enantioselectivity but improved rates relative to free cofactor [85]. Cofactor

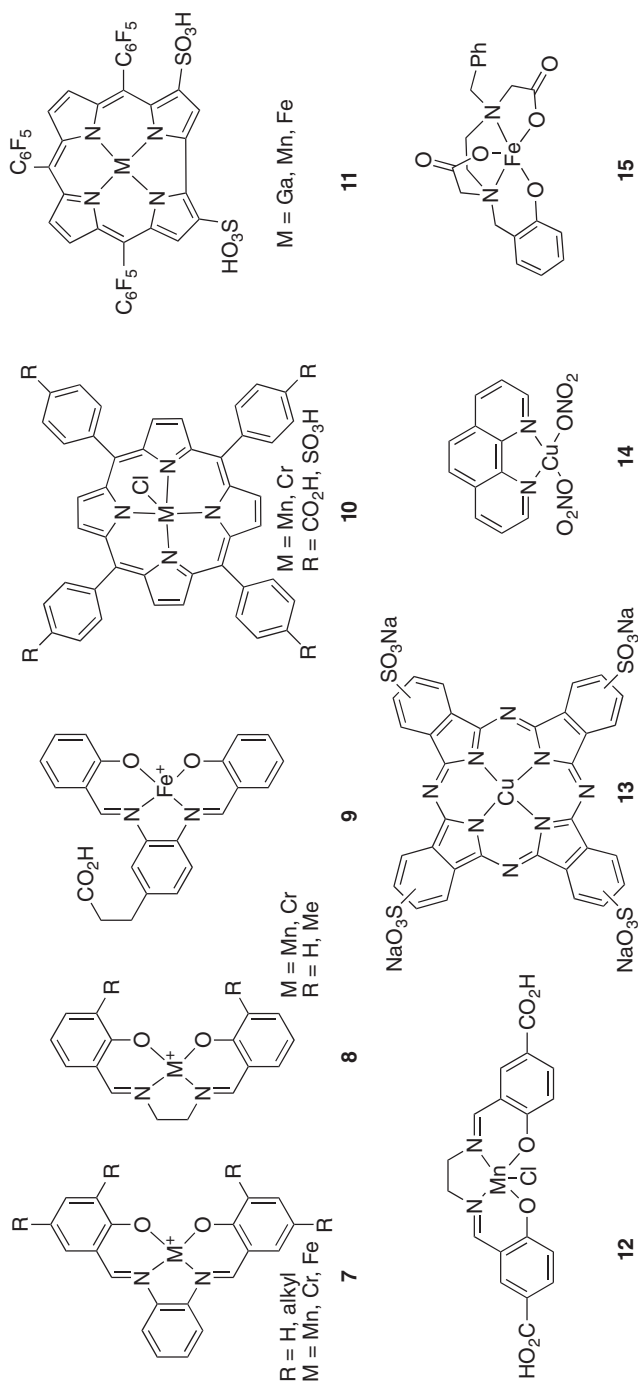


Figure 1.7 Representative structures of cofactors used for ArM formation via cofactor binding.

incorporation was established by ESI-MS, and His ligation of the metal center was suggested by UV/Vis spectroscopy and EPR spectroscopy. His ligation was later observed in the crystal structure of a related Fe–salophen cofactor bound to the active site of myoglobin [86]. This crystal structure also suggested cofactor modifications that could be made to improve binding with the myoglobin scaffold. Mn(III) and Cr(III) salen complexes bearing pendant alkyl groups (**8**, Figure 1.7) were therefore incorporated into myoglobin, and crystallographic characterization indicated that cofactor substitution could indeed be used to alter its orientation. Moreover, substituted cofactors led to altered and even inverted enantioselectivity in ArM-catalyzed sulfoxidation reactions [87]. Yields for these systems were typically low (<10%), although up to 30% could be obtained in some cases.

Hartwig generated a family of ArMs by reconstituting apo-myoglobin with protoporphyrin IX cofactors containing several different metals. In this case, apo-myoglobin was purified prior to metalation unlike the previous report by Watanabe [79], which was reported to allow quantitative metalation using stoichiometric cofactor. Cofactor incorporation was confirmed by ESI-MS, and a (PPIX)Ir(Me) ArM was found to catalyze olefin epoxidation and intramolecular C–H insertion of diazo substrates with high enantioselectivity (up to 82% *ee* and 86% *ee*, respectively) as a result of mutations targeted to the myoglobin active site [88].

Heme oxygenases have also been used as scaffolds for ArM formation due to their facile reconstitution with artificial heme-like cofactors. These enzymes catalyze the conversion of heme to biliverdin using reducing equivalents provided by an electron transfer network originating from a cytochrome p450 reductase. Watanabe demonstrated that HO from *Corynebacterium diphtheriae* could be reconstituted with a variety of Fe(III)–salophen derivatives (**9**; Figure 1.7) to produce ArMs that retained their ability to interface with their native electron transfer partners to reduce O₂ to superoxide [89]. ESI-MS was used to confirm cofactor incorporation, and X-ray crystallography revealed that the salophen cofactors were indeed held in the native heme binding site [90]. This crystal structure enabled structure-based design of complexes that could improve ArM stability. Recently, the artificial HO–salophen system was subjected to a detailed mechanistic study to reveal the perturbed resting state of the ArM-catalyst relative its native parent [91].

1.3.1.2 Xylanases

Xylanases have been explored as host scaffolds for the formation of artificial hemoproteins due to the depth of their substrate-binding clefts and their availability from thermophilic source organisms. One early report showed that both *Thermotoga maritima* xylanase B (TMX), exhibiting an (α/β)₈ TIM-barrel fold, and the catalytic domain of *Dictyoglomus thermophilum* xylanase B (DTX), exhibiting a β -jelly roll fold, can form 1:1 adducts with a synthetic iron-containing porphyrins bearing a pendant axial histidine ligand, although no catalysis was reported [92]. On the other hand, Mahy was able to incorporate simple carboxylate-substituted iron porphyrins (e.g., **10**; Figure 1.7) into the catalytic domain of xylanase A from *Streptomyces lividans* to

generate an ArM peroxidase. Nanomolar porphyrin binding was established via spectrophotometric titration, and an isosbestic change in the UV/Vis spectrum was hypothesized to arise due to axial coordination of the metal by a scaffold residue. ArM peroxidase activity toward guaiacol and *o*-dianisidine in the presence of H₂O₂ was lower but longer lived than that of free cofactor, ultimately providing greater yields of oxidized products. The improved lifetime of the ArM was attributed to sequestration of the porphyrin catalyst inside a protein scaffold, minimizing oxidation by reactive species generated during catalysis [93]. This ArM also catalyzed sulfoxidation of thioanisole with modest enantioselectivity in the presence of an imidazole cocatalyst, and switching the porphyrin metal from iron to manganese enabled alkene epoxidation activity [94]. Characterizing Mn-porphyrin binding was complicated by the lack of a spectral shift upon cofactor binding, so fluorescence quenching of endogenous tryptophans was used. Low micromolar binding was observed, and the resulting ArM catalyzed styrene epoxidation in the presence of KHSO₅ with up to 80% *ee* [95].

1.3.1.3 Serum Albumins

The versatility of serum albumins as scaffolds for ArM formation via metal binding was noted in Section 1.2.2, and these remarkable proteins can also bind a range of metal complexes to generate ArMs [30]. The known heme-binding capability of albumins naturally led to a number of studies on ArM formed from heme and heme-like cofactors. One of the first reports leveraged heme binding to direct a carboxylate-substituted manganese porphyrin into BSA, where it was covalently grafted to the scaffold via peptide bond formation. This ArM was then applied for the enantioselective dioxygenolysis of a racemic tryptophan–peroxide derivative [96]. Since this early report, researchers have recognized that supramolecular binding of heme-type complexes tends to be tight enough to obviate the need for covalent linkage.

For example, Gray reported a detailed spectroscopic study of HSA binding to amphiphilic Ga(III)- and Mn(III)-corrole cofactors (**11**; Figure 1.7) [97]. Changes in the UV/Vis Soret band upon titration of HSA into solutions of the corroles indicated strong association of the complex to the protein, which was corroborated by coelution of corrole and HSA by HPLC. Strong Cotton effects were observed in the CD spectra, particularly for absorbances related to axial ligation of the metalated corrole. Tryptophan fluorescence quenching (HSA has only a single tryptophan) was used to determine that HSA exhibits nanomolar binding affinities for the corroles, and Förster resonance energy transfer (FRET) experiments were used to approximate the location of the complex in HSA [97]. These findings were later applied to generate ArMs from Fe- and Mn-substituted corroles bound to a panel of human, rabbit, pig, sheep, and BSA. These ArMs converted prochiral thioethers to their corresponding sulfoxides in the presence of H₂O₂ or iodosylbenzene with good enantioselectivity [98].

The crystal structure of hemin-bound HSA revealed that the cofactor bound to the protein through non-covalent electrostatic interactions of Arg114, His146, and Lys190 with the negatively charged carboxylates of protoporphyrin IX, as well as through weak coordination of the iron center by Tyr161 [99]. A series of studies have sought to explore the potential for this system to mimic the chemistry of

various hemoproteins [92]. In particular, an engineered HSA was used to generate an ArM peroxidase that catalyzed the one-electron oxidation of phenols [100], and an ArM superoxide dismutase was generated using a Mn–protoporphyrin IX cofactor. Cofactor binding was confirmed by UV/Vis spectroscopy, and the site of Mn(PPIX)-binding was presumed to occur at the same site for Fe(PPIX) given spectral shifts upon mutation of Tyr161 to leucine [101].

Metal salen and salophen cofactors have also been used to generate ArMs from serum albumins. Ménage used ICP-MS to determine that up to four Mn(salen) complexes (**12**; Figure 1.7) were incorporated into HSA, depending on the equivalents of cofactor used [102]. As in the aforementioned work by Gray, tryptophan fluorescence quenching and CD spectroscopy were used to provide additional insight into cofactor binding. The resulting ArM catalyzed sulfide oxidation, and while no enantioselectivity was observed, conversion and chemoselectivity for sulfoxide versus sulfone formation were increased relative to the small-molecule catalyzed reaction. This was attributed to the hydrophobicity of the environment around the HSA-bound catalyst, driving the partially oxidized sulfoxide product away into bulk solution before complete oxidation to the sulfone could take place [102]. Similar methods and characterization were reported for an ArM superoxide dismutase generated using an Mn(salophen) cofactor [103] and an ArM sulfoxidase generated using a Co(salen) cofactor. In the latter case, chemoselectivity for sulfoxidation was again improved relative to free cofactor as observed by Ménage, and up to 85% *ee* could be obtained for select substrates [104].

Outside of the redox catalytic manifold typically explored with serum albumin/heme-like complexes, Reetz demonstrated that Cu(II)–phthalocyanine cofactor **13** (Figure 1.7) could bind to various serum albumins, in some cases generating highly enantioselective catalysts for Diels–Alder reactions of azachalcones with cyclopentadiene (>90% *ee*). Binding of the complex to BSA was confirmed by MALDI-MS and by the emergence of new UV/Vis spectral features upon mixing the complex with the protein scaffold [105].

1.3.1.4 Lactococcal Multidrug Resistance Regulator

Recently, Roelfes reported the supramolecular assembly of a Cu(II)–phenanthroline cofactor **14** (Figure 1.7) to the interfacial cavity of the dimeric LmrR [106]. The hydrophobic cavity generated upon dimer formation was exploited as a viable site for binding planar coordination complexes. A scaffold mutant that provided improved expression was used to bind a variety of Cu(II) complexes supported by bidentate aromatic nitrogen ligands. Tryptophan fluorescence quenching was used to quantitate cofactor binding affinity ($K_d \sim 0.7\text{--}8.5\ \mu\text{M}$). The resulting ArMs catalyzed Friedel–Crafts alkylation of a variety of indoles with >90% *ee*. Negligible enantioselectivity of an ArM generated via mutagenesis of an interfacial tryptophan (W96A) required for dimerization and fluorescence lifetime experiments supported cofactor binding at the dimer interface.

1.3.1.5 Nika

Ménage and Fontecilla-Camps have developed a series of ArMs based on the periplasmic nickel-binding protein Nika from *Escherichia coli*. A crystal

structure of this protein indicated the presence of bound $\text{Fe}^{\text{III}}(\text{EDTA})$ from the periplasmic extraction procedure to isolate the overexpressed protein. The identity of this complex was confirmed X-ray crystallography, X-ray fluorescence, and electrospray ionization MS [107]. Given the similarity of EDTA complexes to many catalysts and the peroxidase activity of $\text{Fe}^{\text{III}}(\text{EDTA})$ itself [108], NikA was explored as an ArM scaffold. Remarkably, an ArM generated from NikA and tetradentate cofactor **15** (Figure 1.7) was examined by X-ray crystallography throughout the course of the O_2 -mediated hydroxylation of the pendant phenyl group of the ligand [109]. While this reaction is stoichiometric, it demonstrates the exciting potential of these hybrid systems to reveal fundamental mechanistic insights into transition metal reactivity. Recently, NikA and a similar $\text{Fe}(\text{II})$ -tetradentate complex were demonstrated to form a competent ArM for the sulfoxidation of a panel of aryl thioethers in the presence of NaOCl . No significant enantioselectivity was observed, but the ArM was able to enhance chemoselectivity toward specific substrates [110].

1.3.1.6 Antibodies

The potential to exploit the binding capabilities of antibodies for catalysis, particularly antibodies raised against transition state analogues, has been extensively explored. Rather than binding substrates, however, antibodies have also been generated for metal ions [111, 112], reactive organic fragments [113, 114], and transition metal catalysts [115], in the latter case leading to ArMs. Reardan and Meares first demonstrated that antibodies could be raised against metal complexes; antibodies CHA255 and CHB235 were found to bind $\text{EDTA-In}(\text{III})$ complexes with high affinity [116]. Lerner then showed that antibody-based ArM proteases could be generated by raising antibodies against trien- $\text{Co}(\text{III})$ -peptide haptens (**16**, Figure 1.8) [117]. An ELISA competition assay indicated that the resulting antibodies bound a number of transition metal trien complexes (**17**, Figure 1.8), including $\text{Zn}(\text{II})$, $\text{Fe}(\text{III})$, $\text{Ga}(\text{III})$, $\text{Cu}(\text{II})$, and $\text{Ni}(\text{II})$, that imparted

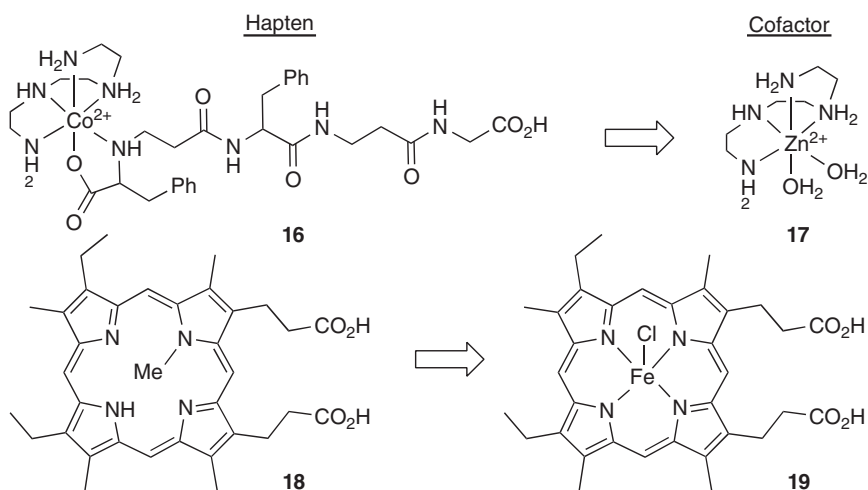


Figure 1.8 Structures of cofactors used for ArM formation via cofactor anchoring.

protease activity to antibody 28F11. Schultz showed that an antibody raised against *N*-methylmesoporphyrin IX (**18**, Figure 1.8) could catalyze metalation of protoporphyrin IV [118] and subsequently found that metalation of this antibody with Fe(III) mesoporphyrin led to the formation of an ArM peroxidase [119] (**19**, Figure 1.8). Characterization of the ArM by UV/Vis spectroscopy showed an increase in the intensity, but no change in the wavelength of the Soret band, consistent with cofactor binding in a hydrophobic environment without axial coordination. Similar approaches have been used to generate ArM peroxidases from Fe(ToCPP) [120, 121], microperoxidase 8 (which possesses a histidine-ligated Fe(III) center) [122], and several other porphyrins [115]. Schultz also developed and used an affinity-based selection strategy to improve the peroxidase activity of antibody-based ArM peroxidases, the first example (predating the Zn(II) ArM noted in Section 1.2.2) of a selection to improve the function of an ArM of any type [123].

1.3.2 Cofactor Anchoring

Binding metal complexes to proteins inherently couples the cofactor structure and thus its chemistry to its ability to bind within the scaffold protein. Modification of the ligand can compromise its ability to bind with the scaffold. To decouple catalyst structure from binding, it can be tethered to a binding element that can anchor it to a suitable scaffold protein (Figure 1.6). While this allows the potential to introduce a range of different metal complexes into a given scaffold, it does limit the range of scaffolds that can be used, and it requires that sufficient interactions between cofactor and scaffold be established despite the presence of a linker (often flexible) between the scaffold and the catalyst.

1.3.2.1 (Strept)avidin

One of the first examples of an ArM of any type involves anchoring biotinylated metal complexes to avidin. The tight binding of biotin to avidin ($K_d \sim 10^{-12} - 10^{-15}$ M) ensures rapid and essentially quantitative ArM formation. Biotin binds such that its terminal carboxylate projects from the biotin binding site, providing a convenient attachment point for metal complexes and ensuring close proximity between the metal complex and the scaffold. Whitesides first showed that this approach could be used to generate an avidin-based hydrogenase using biotinylated Rh–bisphosphine complex **20** (Figure 1.9) [124]. Chan later demonstrated that avidin binding could alter and even invert the enantioselectivity of chiral biotinylated Rh–pyrphos complexes (**21**, Figure 1.9) [125]. More recently, Ward has exploited the binding of both avidin and streptavidin to biotin-substituted cofactors (e.g., **22–26**, Figure 1.9) to prepare a wide range of ArMs with high selectivity and activity for a variety of reactions, including transfer hydrogenation [126], olefin metathesis [127], and cross-coupling [128]. A variety of experimental and computational techniques have been used to characterize these ArMs, providing a wealth of information on ArM structure and design [129–131]. Particularly notable observations include resolution of racemic, chiral-at-metal complexes within ArM active sites [132], several examples of scaffold accelerated catalysis [38], and instances in which

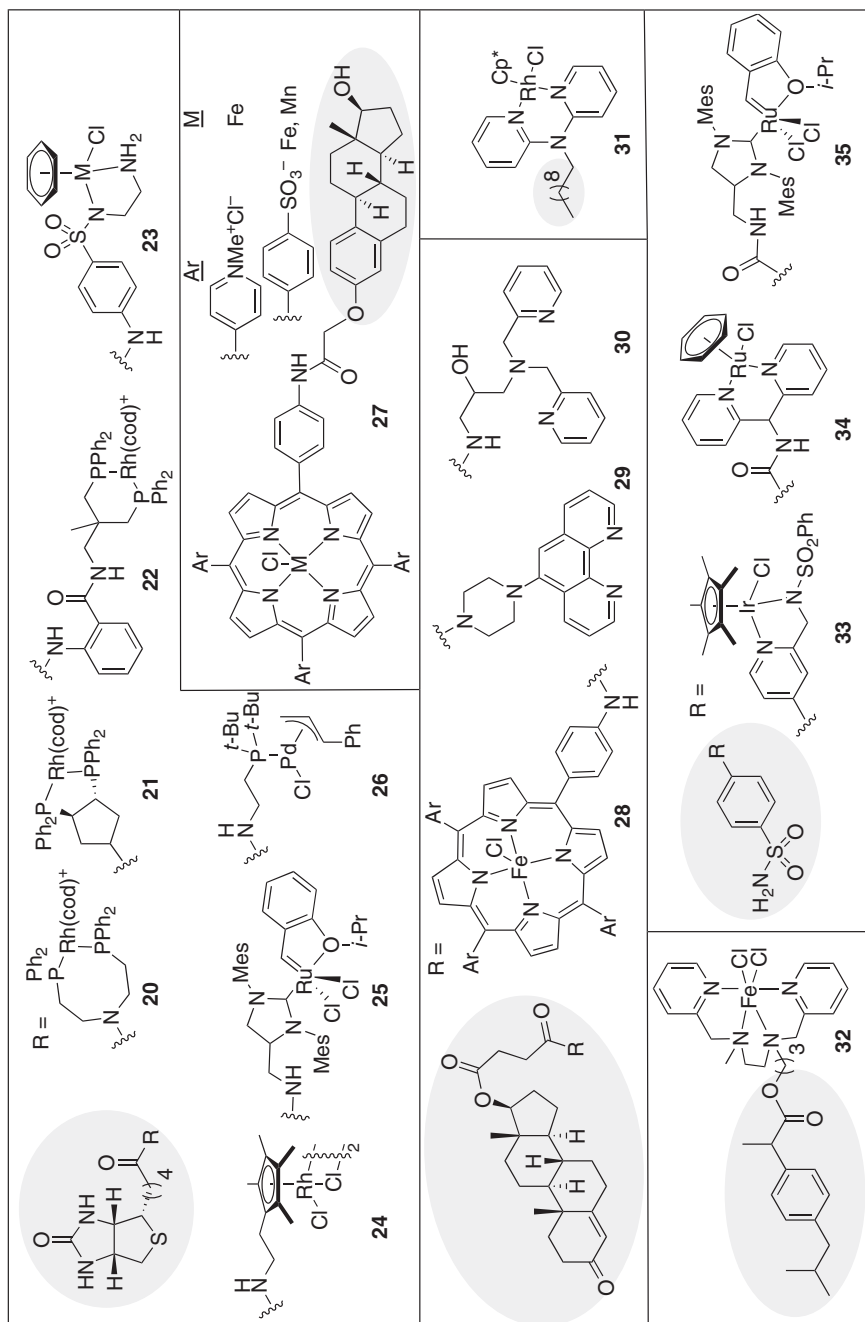


Figure 1.9 Structures of cofactors used for ArM formation via cofactor anchoring. Anchoring groups are highlighted in grey.

scaffold residues bind to the metal center [133] or potentially facilitate reactions at the metal center [134]. Equally exciting are the numerous applications that these ArMs are now enabling, including ArM evolution [135] and tandem catalysis [136].

1.3.2.2 Other Anchoring Scaffolds

Based on the success of this system, a number of related anchoring strategies have also been pursued. Essential to all of these is the identification of a high affinity interaction between a scaffold and an anchor that can be tethered to a metal complex of interest. Given the known affinity of antibodies for their respective antigens, it is perhaps not surprising that an antibody scaffold was first used to broaden the anchoring approach beyond (strept)avidin–biotin systems. Specifically, antibody 7A3, which has high affinity for estradiol, was used by Mahy and coworkers to generate an ArM with peroxidase and sulfoxidase activity using estradiol-substituted Fe- and Mn-porphyrin cofactors (**27**, Figure 1.9) [137–139]. Subsequent work showed that a neocarzinostatin variant evolved to bind testosterone could be used to generate ArMs from testosterone-substituted Fe(III), Zn(II), and Cu(II) cofactors **28–30** (Figure 1.9) [140–142]. Similarly, ibuprofen-substituted Fe(II) cofactor **32** (Figure 1.9) was bound to NikA to generate an ArM sulfoxidase [143], a heme-substituted bipy cofactor that was used to reconstitute myoglobin to generate an ArM Diels–Alderase following metalation with Cu(II) [144] and acylated 2,2-dipyridylamine cofactor **31** (Figure 1.9) was bound to β -lactoglobulin to generate an ArM transfer hydrogenase [145]. For each of these systems, low enantioselectivity was reported for catalytic transformations (where relevant), micromolar cofactor binding was observed, and while cofactor binding was typically established using spectroscopic methods (UV/Vis, EPR, CD, etc.), the location of the metal center within the ArM was not established. ArM yields following purification and extent of cofactor dissociation during the course of ArM catalysis are rarely provided for these systems or those generated via direct cofactor binding [143, 146], which could account for the low selectivity observed in many cases.

1.3.2.3 Carboxyanhydrase

Greater success has been obtained using ArMs generated from carboxyanhydrase. This enzyme is known to bind aryl sulfonamides with high affinity, and Ward found that several aryl sulfonamide-substituted cofactors (e.g., **33**, **34**, Figure 1.9) bound to carboxyanhydrase to generate ArMs transfer hydrogenases with good enantioselectivity [147, 148]. The crystal structure of one of these ArMs clearly showed the metal center within the entrance of the substrate binding pocket of the CA scaffold, although partial metal dissociation from the cofactor was suggested by the fact that the diffraction data were best modeled using 50% occupancy of the $[(C_6H_6)_2RuCl]$ fragment of **34** (Figure 1.9). Computational design was recently used to improve cofactor binding (K_d as low as 0.33 nM), leading to ArMs that catalyzed transfer hydrogenation that significantly improved enantioselectivity ($>90\%$ *ee*) [149]. Grubbs–Hoveyda-type olefin metathesis catalyst **35** (Figure 1.9) was also incorporated into hCA via this approach, and nanomolar cofactor binding was observed [146].

1.4 ArM Formation via Covalent Linkage

While supramolecular anchoring strategies expand the range of cofactors that can be incorporated into protein scaffolds, they require scaffolds that bind particular anchors, which limit the range of scaffolds that can be used for ArM formation. As noted above, cofactor dissociation under conditions optimal for catalysis (rather than ArM formation) can also lead to nonselective background reactions for these systems. Researchers have therefore explored covalent methods to install synthetic catalysts and ligands that can be subsequently metalated into a broader range of scaffolds (Figure 1.10) [1, 150]. This approach provides great flexibility to exploit the previously noted possibility of selecting scaffolds that might possess inherent functionality that can be exploited for ArM catalysis. ArM nucleases generated from DNA-binding scaffolds nicely illustrate this type of exaptation [151], but even providing a more suitable enclosure for bulky catalysts can constitute a major advantage for using a particular scaffold for ArM formation [4].

Covalent ArM formation benefits immensely from the large amount of bioconjugation methodology available in the literature [152], but several aspects of ArM formation, first noted in Section 1.2, present unique challenges to these methods [1]. Site-specific cofactor incorporation requires that suitably reactive residues (lysine, cysteine, etc.) be introduced, and any residues with similar reactivity toward a target linkage site must be removed [153]. The site of modification must typically be located at a scaffold position that will situate the metal center within rather than projecting from the scaffold to impart selectivity to the cofactor [43]. This can be challenging for many bioconjugation methods, which are typically optimized using reactions of readily accessible surface residues rather than residues buried in scaffold clefts or barrels [152]. Moreover, while long flexible linkers are typically used for many bioconjugation applications, this flexibility can lead to cofactor movement in the context of an ArM, so minimizing linker length and flexibility is important. Finally, evolution of covalent ArMs, described in detail later in this book, requires rapid, high-yielding bioconjugation reactions that are compatible with cell lysate [154], which precludes the use of many classical bioconjugation reactions. Despite these challenges, a number of methods have been developed to enable broad exploration of covalent ArMs [1, 150].

1.4.1 Activated Serine and Cysteine Residues

Kaiser first reported that synthetic cofactors could be covalently linked to scaffold proteins to generate artificial enzymes by exploiting the native activity of papain (Table 1.1, entry 1) [155, 156]. The unique nucleophilicity of the active site cysteine of papain allowed for its selective alkylation using α -haloketone-substituted

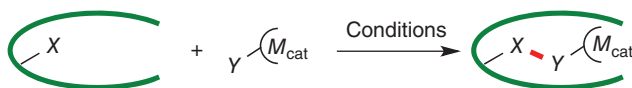
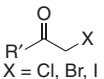
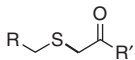
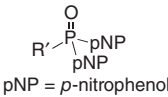
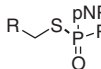
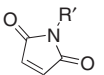
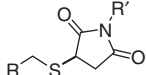
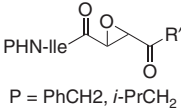
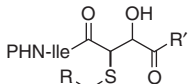
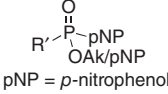
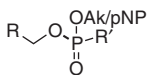
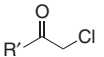
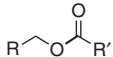


Figure 1.10 General scheme for ArM formation via covalent linkage.

Table 1.1 Covalent modification of hydrolase scaffolds.

Entry	X (residue)	Y	X-Y
1 [155, 156]	R-SH (Papain)		
2 [157]	R-SH (Papain)		
3 [157]	R-SH (Papain)		
4 [158]	R-SH (Papain)		
5 [159, 160]	R-OH (Serine hydrolase)		
6 [161]	R-OH (Serine hydrolase)		

flavins (e.g., **36**, Figure 1.11). Chemoselective bioconjugation was confirmed by measuring loss of scaffold hydrolase activity, and this method was used in subsequent efforts toward ArM formation. Early examples established that phosphonate-substituted bisphosphine **37**, maleimide-substituted Mn-salen (**38**, Figure 1.11), and Cu-, Pd-, and Rh-bipyridine cofactors (**39**, Figure 1.11) [157], in addition to phosphite **40** (Figure 1.11), which was subsequently metalated by [Rh(COD)]⁺ [162], could all be covalently linked to papain (Table 1.1, entries 1–3, Figure 1.11). Unfortunately, low catalytic efficiency and selectivity was reported for each of these systems, and only the latter confirmed incorporation of the metal fragment via mass spectrometry. Significantly better catalytic efficiencies were obtained for several papain-based Diels–Alderases [163] and transfer hydrogenases [164, 165], and the selectivity of the latter has been improved by designing cofactors (**41**, Figure 1.11) with affinity for the S1 (protease subsite nomenclature) substrate binding subsite of papain (Table 1.1) [158]. These more recent examples confirm not only high levels of bioconjugation via loss of hydrolase activity but also incorporation of only a single cofactor by mass spectrometry or UV/Vis spectroscopy.

Further exploiting the native activity of hydrolases, van Koten demonstrated that phosphonate-substituted metallacycles (e.g., **42**, Figure 1.11) could be covalently linked to cutinase, a serine hydrolase (Table 1.1, entry 5) [159, 160]. Recently, the phosphonate linkage approach was used to generate ArMs from *Candida antarctica* lipase B (CALB) or cutinase that catalyze olefin metathesis [166], hydrogenation [167], and Heck reaction [168]. An

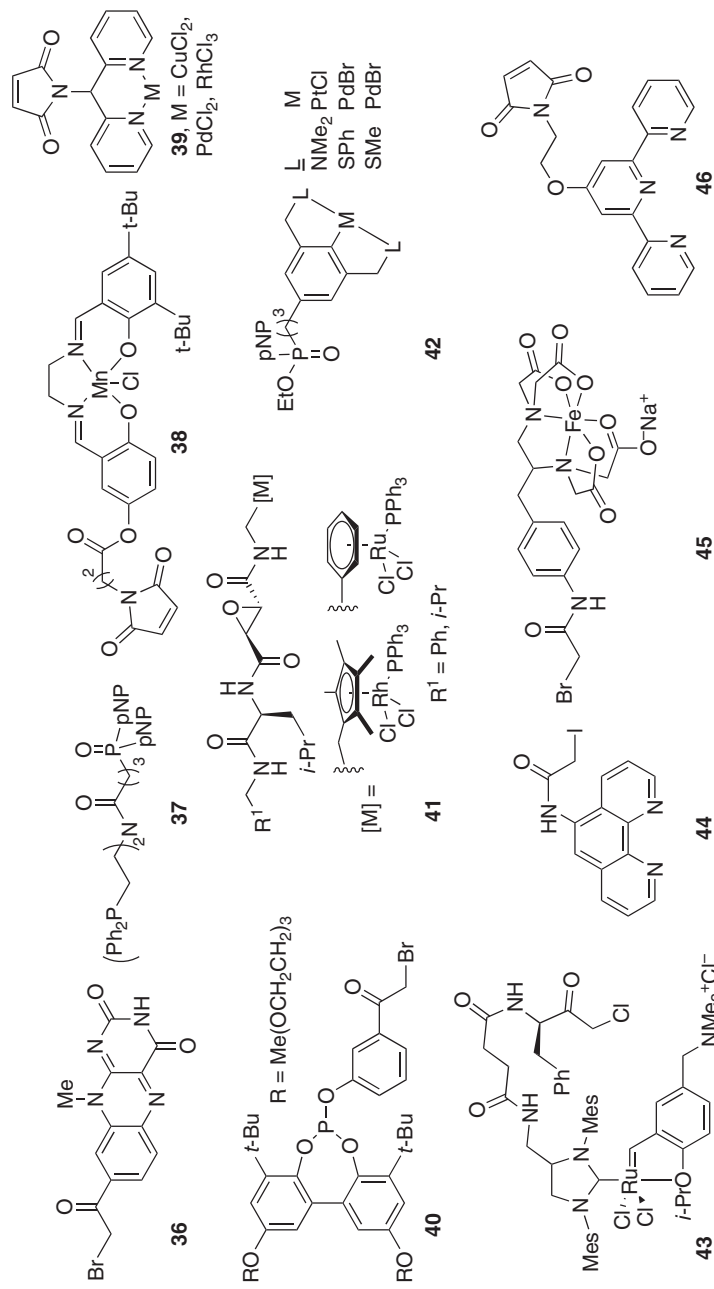


Figure 1.11 Representative covalent ArM cofactors.

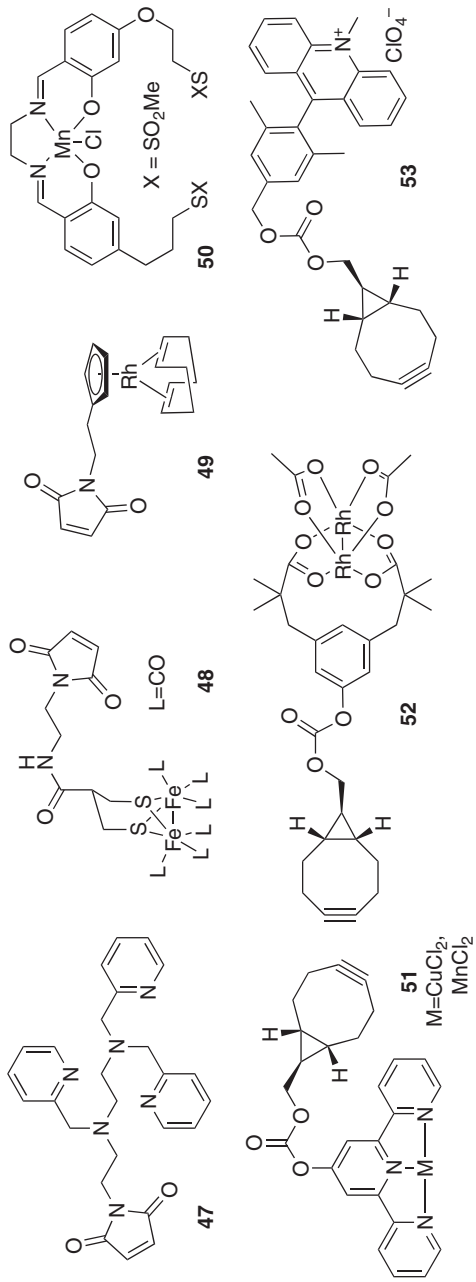


Figure 1.11 (Continued)

ArM-catalyzed Heck reaction that proceeded in >90% yield and >90% *ee* was presented in the final example [168]. An ArM that catalyzes olefin metathesis was also generated via alkylation (Table 1.1, entry 6) of α -chymotrypsin with an α -haloketone-substituted Grubbs–Hoveyda catalyst with S1 subsite binding capability (**43**, Figure 1.11) [161]. Bioconjugation conversion in each of these cases was again established by confirming loss of scaffold activity, and in most cases MS data were provided to establish addition of a single cofactor.

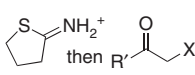
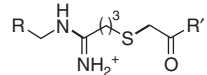
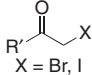
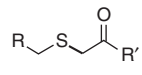
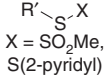
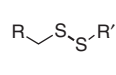
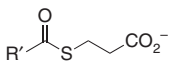
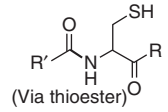
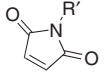
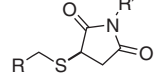
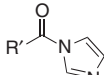
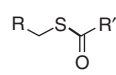
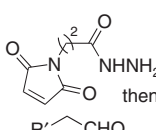
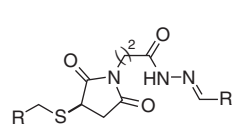
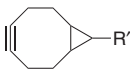

1.4.2 Lysine Residues

While the selectivity by which active site cysteine and serine residues in hydrolase scaffolds can be modified eliminates the need for installing reactive residues for scaffold bioconjugation, it also leads to limitations in scaffold scope similar to those discussed for supramolecular anchoring methods. One of the earliest examples of covalent ArM formation that did not require the unique reactivity of a hydrolase scaffold involved iminothiolane alkylation of surface lysine residues on the *E. coli* Trp repressor protein (*trp*) followed by alkylation of the resulting thiol with [³H]5-iodoacetamide-1,10-phenanthroline (**44**, Figure 1.11) and metalation with Cu(II) (Table 1.2, entry 1) [169]. Of course, extent of bioconjugation in this system and those described below cannot be determined via loss of activity, so alternate means of characterization are required. In the current case, this was achieved using the [³H] radiolabel on the cofactor. Despite the fact that the resulting ArM contained four phenanthroline sites (one for each lysine in *trp*), it catalyzed site-specific cleavage of DNA fragment containing the *aroH* transcription unit naturally recognized by the *trp* scaffold in the presence of Trp and 3-mercaptopropionic acid. Lysine modification using iminothiolane was subsequently used to link an Fe(III)-EDTA cofactor (**45**, Figure 1.11) to the σ^{70} subunit of *E. coli* RNAP complex to generate an ArM that cleaved sites on both nucleic acids and proteins proximal to σ^{70} binding sites [181]. In this case, the extent of bioconjugation varied from 0.6 to 5 equiv. of **45** per scaffold as determined by comparison with authentic standards.

1.4.3 Cysteine Residues

The relative nucleophilicity of cysteine has led to its widespread use for covalent ArM formation. For example, haloacetamide-substituted phenanthroline [173] or EDTA ligands [174] and Fe(III)-EDTA cofactor **45** [175] (Figure 1.11) have been used to generate ArMs for selective biopolymer cleavage with activities analogous to those noted above without the need to for iminothiolane treatment (Table 1.2, entry 2) [150]. An optimized protocol [175] for incorporating cofactor **45** provides a nice overview of relative cysteine reactivity toward this cofactor, describes conditions for assaying free cysteine residues (and thus extent of bioconjugation), and shows MS data showing selective mono addition to a representative scaffold protein. Disulfide exchange [177] and transesterification (followed by intramolecular rearrangement to form an amide bond) [178] have also been used to incorporate related triacetate ligands into proteins to generate ArMs following metalation with Fe(III) (Table 1.2, entries 3 and 4). In the latter case,

Table 1.2 Covalent modification of amino acids.

Entry	X (residue)	Y	X-Y
1 [169]	R-CH ₂ NH ₂ (Lysine)		
2 [72, 162, 170–175]	R-CH ₂ SH (Cysteine)		
3 [176, 177]	R-CH ₂ SH (Cysteine)		
4 [178]	R-CH ₂ SH (Cysteine)		
5 [153, 157, 163, 164]	R-CH ₂ SH (Cysteine)		
6 [179]	R-CH ₂ SH (Cysteine)		
7 [180]	R-CH ₂ SH (Cysteine)		
8 [3]	R-N ₃ (<i>p</i> -Azidophenylalanine)		

only *N*-terminal cysteine residues are labeled due to the required rearrangement, and regeneration of the cysteine residue following bioconjugation was confirmed by secondary labeling with 4-vinyl pyridine followed by MS and amino acid analysis.

The cleavage reactions catalyzed by the Fe(III) ArMs outlined above proceed via diffusible hydroxyl radicals and can therefore occur at sites distal to the metal center [181]. While this mechanism is amenable to selective biopolymer cleavage [150, 182], alternate oxidation catalysts could be used to provide greater control over these oxidation reactions. Indeed, processive DNA cleavage was recently achieved using an ArM generated by linking a maleimide-substituted Mn porphyrin to a cysteine mutant of T4 sliding clamp protein [183]. In this case, the scaffold protein formed a trimeric quaternary structure with 1.4 cysteine residues/trimer available for bioconjugation according to Ellman's assay. Complete bioconjugation of these sites (1.3–1.4/trimer) was indicated by UV/Vis spectroscopy and the Bradford assay, and similar Soret bands for the free and bioconjugated cofactor suggested the absence of scaffold binding to the

Mn center. The Mn-oxo intermediate generated by treating the resulting ArM with KHSO_5 cleaves only sequences that contain three consecutive A-T base pairs, making it considerably more selective than the diffusible oxidants used in the systems outlined above.

Distefano first explored the potential for ArMs generated via cysteine modification to be used for enantioselective catalysis. Specifically, adipocyte lipid-binding protein (ALBP), which contains a single cysteine residue within a large (600 \AA^3) cavity, was used as a scaffold for covalent attachment of **44** (Figure 1.11, Table 1.2, entry 2) [170]. Bioconjugation ($\sim 90\%$ conversion) was characterized via 5,5'-disulfaneylbis(2-nitrobenzoic acid) (DTNB) thiol titration, MS, and UV/Vis spectroscopy. Metalation of the resulting bioconjugate with Cu(II) was characterized by phenanthroline fluorescence quenching, and the resulting ArM catalyzed amide hydrolysis and enantioselective ester hydrolysis. High enantioselectivity ($>90\%$ ee) and modest TONs were observed for the kinetic resolution of amino acid esters [184], and the crystal structure of the ArM showed little structural perturbation of the scaffold despite complete encapsulation of the cofactor [185].

A broad range of metal complexes and ligands have subsequently been used to generate ArM constructs via cysteine modification with maleimide-substituted cofactors (Table 1.2, entry 8). Reetz demonstrated that a maleimide-substituted phenanthroline ligand could be used to alkylate cysteine residues introduced into the interior of tHisF [153]. The Lewis [5] and Mahy [145] groups incorporated maleimide-substituted tri- and tetradentate nitrogen ligands (Figure 1.11, **46** and **47**) into the interior of tHisF, nitrobindin, and β -lactoglobulin to generate ArM peroxygenases following metalation with Mn and Fe, respectively. Several groups have incorporated Grubbs–Hoveyda catalysts into proteins. In addition to the cutinase [166], α -chymotrypsin [161], and carboxyanhydrase [146] systems noted above, cysteine mutants of a small heat shock protein [171] and FhuA [186] have been alkylated with maleimide- and α -haloketone-substituted Grubbs–Hoveyda catalysts to generate ArMs that catalyze olefin metathesis. While ArM-catalyzed polymerization remains rare, Bruns has used cysteine alkylation to incorporate ATRP catalysts into protein cage scaffolds [187], and Hayashi showed that a cysteine mutant of nitrobindin could be alkylated with maleimide-substituted piano stool Rh cofactor **48** (Figure 1.11) to generate an ArM that catalyzed alkyne polymerization [188]. Nitrobindin was later alkylated with maleimide-substituted diiron complex **49** (Figure 1.11) to generate an ArM that, upon irradiation in the presence of $[\text{Ru}(\text{bpy})_3]^{2+}$ and ascorbate in aqueous solution, reduced protons to H_2 [189]. A number of biohybrid photosynthetic antenna systems have also been prepared via covalent attachment of chromophores to cysteine mutants of photosynthetic proteins [190, 191]. Methods to incorporate phosphorous-based ligands into proteins via cysteine modification with non-maleimide-based chemistry to enable ArM formation following metalation have also been reported (Table 1.2, entries 6 and 7) [179, 180].

Remarkably, in all of these cases after the early work of Distefano, little if any enantioselectivity or regioselectivity was observed in reactions where such selectivity is possible. The reasons for this are likely manifold for each system, but

nonselective or multiple cofactor additions, insufficient cofactor encapsulation, cofactor movement within the ArM, and poor substrate binding have been proposed to contribute [1, 162]. Unlike cofactor binding or anchoring methods, non-covalent interactions that might orient cofactors within an active site are not required for covalent ArM formation, meaning that such interactions are either fortuitous or must be introduced *de novo*. Characterization of these systems typically includes thiol titration to establish extent of cysteine bioconjugation (often >90%) and MS to establish that the major product contains a single cofactor molecule, but experimental evidence showing a lack of multiple cofactor additions [145] is less commonly presented. Because many methods, including ICP-MS and UV/Vis spectroscopy, cannot distinguish between high levels single site cofactor bioconjugation and low levels of nonselective bioconjugation (assuming, in the latter case, that no unique spectral features result from ArM formation), multiple methods must be used to establish that the extent of bioconjugation is equivalent to the amount of bulk metal in the system [170, 171, 175]. In addition, as previously noted for ArMs generated via supramolecular anchoring, few studies have definitively established encapsulation within the protein scaffolds used, and in many cases, the linker lengths used (Figure 1.11) likely lead to cofactor projecting out of the scaffold [3]. To address the cofactor movement issue, however, Lu examined dual-point attachment of doubly methane thiosulfonate-substituted Mn-salen complex **50** (Figure 1.11) to a cysteine double mutant (L72C/Y103C) of apo-myoglobin (apo-Mb) and observed improved selectivity for thioanisole sulfoxidation relative to the analogous single point mutant (Table 1.2, entry 3) [176]. This result clearly established that improved cofactor binding can improve ArM selectivity, as did later work by Ward [149] and Lewis [4].

Roelfes demonstrated that cysteine residues installed at the hydrophobic dimer interface of the dimeric transcription repressor LmrR could be alkylated using phenanthroline **44** (Figure 1.11) to generate ArMs following metalation with Cu(II) [172]. Notably, this scaffold completely encapsulates the cofactor, just as the early example from Distefano. The resulting ArMs catalyze both the Diels–Alder reactions between azachalcones and cyclopentadiene and hydration of azachalcones with high enantioselectivity (>90% *ee*). Filice later showed that high levels of enantioselectivity (>90% *ee*) for the same Diels–Alder reaction can be obtained from ArM generated via covalent attachment of **44** to cysteine mutations introduced into *G. thermocatenulatus* lipase in a pocket distal to the lipase active site [168]. Interestingly, this ArM was generated using immobilized scaffold, and the native hydrolase activity of the scaffold remained operative following ArM formation.

1.4.4 Azido Phenylalanine

As noted above, cysteine mutations can be readily introduced into proteins to enable bioconjugation of a wide range of cofactors, but any additional residues that react under alkylation conditions used must also be removed [153], which is time-consuming and can be problematic if these residues are structurally important. Moreover, these reactions require the use of purified scaffold proteins rather

than crude scaffolds in cell lysate unless a large excess of cofactor is used. This would complicate the use of library approaches for ArM evolution [192].

Lewis therefore demonstrated that bicyclononyne-substituted cofactors could be incorporated into scaffolds containing a genetically encoded *p*-azidophenylalanine residue via strain-promoted azide–alkyne cycloaddition (Table 1.2, entry 8) [3]. The bioorthogonal strain-promoted azide–alkyne cycloaddition (SPAAC) reaction eliminates the need to remove native amino acid residues in the scaffold and facilitates ArM formation under a variety of reaction conditions [154]. Bicyclo[6.1.0]nonyne (BCN)-substituted Mn- and Cu-terpyridine (**51**, Figure 1.11) and dirhodium-tetracarboxylate (**52**, Figure 1.11) cofactors could all be incorporated into different scaffold proteins using this approach. An optimized dirhodium ArM generated from a *Pfu* prolyl oligopeptidase scaffold catalyzed cyclopropanation of *p*-methoxystyrene using ethyl diazoacetate with high enantioselectivity (>90% *ee*) [4]. Use of a scaffold from a hyperthermophilic organism greatly facilitated ArM preparation, purification, and mutagenesis. As with the xylanase-based ArM peroxidase noted above [93], lower but longer-lived activity was observed for POP-based dirhodium ArMs relative to free cofactor, presumably due to cofactor sequestration in the ArM active site. Lewis later showed that similar incorporation of acridinium chromophore **53** (Figure 1.11) into a cysteine mutant of *Pfu* prolyl oligopeptidase could be used to generate an artificial enzyme that catalyzes thioether sulfoxidation [193]. In all of these cases, bioconjugation yields (typically ranging from 50% to 100%) were confirmed by high resolution mass spectrometry (HRMS); variable extent of azide reduction to aniline was responsible for the incomplete conversion.

1.5 Conclusion

The results highlighted above provide a comprehensive summary of methods used to generate ArMs to date. Metal binding, supramolecular interactions, and covalent linkages each provides unique opportunities to study how protein scaffolds can influence the reactivity and selectivity of metal centers. Indeed, examples of ArMs generated via each of these methods that catalyze organic reactions with high enantioselectivity, regioselectivity, or chemoselectivity were presented, although this remains the exception rather than the rule. The utility of natural enzymes for synthetic chemistry has arisen largely as a result of directed evolution efforts to improve their selectivity, activity, and stability for nonnative reactions [194]. Moving forward, it is clear that directed evolution of ArMs will be required if they are to achieve a similar level of utility [135]. Methods for ArM formation that are compatible with library methods and directed evolution schemes (covered later in this book) must therefore be developed. While rational design of ArMs has proven successful in some cases, such efforts are often complicated by the lack of detailed structural information regarding ArM active sites. More detailed characterization of ArMs, particularly via X-ray crystallography, would help in this regard, as would *in situ* and post-reaction

analysis to determine how ArM metalation and modification vary over time. This, combined with improved computational design tools [195], will greatly facilitate optimization of ArMs for synthetic applications.

Acknowledgments

This work was supported by, or in part by, the US Army Research Laboratory and the US Army Research Office under contract/grant number 62247-LS and the NSF (CHE-1351991). K.E.-G. was funded by an NIH Chemistry and Biology Interface Training Grant (T32 GM008720).

References

- 1 Lewis, J.C. (2013) *ACS Catal.*, **3**, 2954–2975.
- 2 Sigman, J., Kwok, B., and Lu, Y. (2000) *J. Am. Chem. Soc.*, **122**, 8192–8196.
- 3 Yang, H., Srivastava, P., Zhang, C., and Lewis, J.C. (2014) *ChemBioChem*, **15**, 223–227.
- 4 Srivastava, P., Yang, H., Ellis-Guardiola, K., and Lewis, J.C. (2015) *Nat. Commun.*, **6**, 1–8.
- 5 Zhang, C., Srivastava, P., Ellis-Guardiola, K., and Lewis, J.C. (2014) *Tetrahedron*, **70**, 4245–4249.
- 6 Key, H.M., Clark, D.S., and Hartwig, J.F. (2015) *J. Am. Chem. Soc.*, **137**, 8261–8268.
- 7 Creus, M., Pordea, A., Rossel, T., Sardo, A., Letondor, C., Ivanova, A., Le Trong, I., Stenkamp, R.E., and Ward, T.R. (2008) *Angew. Chem. Int. Ed.*, **47**, 1400–1404.
- 8 Yoon, T.P. and Jacobsen, E.N. (2003) *Science*, **299**, 1691–1693.
- 9 Ragsdale, S.W. (2006) *Chem. Rev.*, **106**, 3317–3337.
- 10 Lewis, J.C., Coelho, P.S., and Arnold, F.H. (2011) *Chem. Soc. Rev.*, **40**, 2003–2021.
- 11 Lu, Y., Berry, S., and Pfister, T. (2001) *Chem. Rev.*, **101**, 3047–3080.
- 12 Yamamura, K. and Kaiser, E.T. (1976) *J. Chem. Soc. Chem. Commun.*, 830–831.
- 13 Greenblatt, H.M., Feinberg, H., Tucker, P.A., and Shoham, G. (1998) *Acta Cryst.*, **54**, 1–17.
- 14 Okrasa, K. and Kazlauskas, R.J. (2006) *Chem. Eur. J.*, **12**, 1587–1596.
- 15 Hakansson, K., Carlsson, M., Svensson, L.A., and Liljas, A. (1992) *J. Mol. Biol.*, **227**, 1192–1204.
- 16 Hakansson, K., Wehnert, A., and Liljas, A. (1994) *Acta Crystallogr. D Biol. Crystallogr.*, **50**, 93–100.
- 17 Fernández-Gacio, A., Codina, A., Fastrez, J., Riant, O., and Soumillion, P. (2006) *ChemBioChem*, **7**, 1013–1016.
- 18 Jing, Q., Okrasa, K., and Kazlauskas, R.J. (2009) *Chem. Eur. J.*, **15**, 1370–1376.
- 19 Jing, Q. and Kazlauskas, R.J. (2010) *ChemCatChem*, **2**, 953–957.

- 20 Shimahara, H., Yoshida, T., Shibata, Y., Shimizu, M., Kyogoku, Y., Sakiyama, F., Nakazawa, T., Tate, S.I., Ohki, S.Y., Kato, T., Moriyama, H., Kishida, K.I., Tano, Y., Ohkubo, T., and Kobayashi, Y. (2007) *J. Biol. Chem.*, **282**, 9646–9656.
- 21 Fujieda, N., Hasegawa, A., Ishihama, K.-I., and Itoh, S. (2012) *Chem. Asian J.*, **7**, 1203–1207.
- 22 Wong, K.K.W. and Mann, S. (1996) *Adv. Mater.*, **8**, 928–932.
- 23 Abe, S., Niemeyer, J., Abe, M., Takezawa, Y., Ueno, T., Hikage, T., Erker, G., and Watanabe, Y. (2008) *J. Am. Chem. Soc.*, **130**, 10512–10514.
- 24 Ueno, T., Abe, M., Hirata, K., Abe, S., Suzuki, M., Shimizu, N., Yamamoto, M., Takata, M., and Watanabe, Y. (2009) *J. Am. Chem. Soc.*, **131**, 5094–5100.
- 25 Abe, S., Hikage, T., Watanabe, Y., Kitagawa, S., and Ueno, T. (2010) *Inorg. Chem.*, **49**, 6967–6973.
- 26 Abe, S., Hirata, K., Ueno, T., Morino, K., Shimizu, N., Yamamoto, M., Takata, M., Yashima, E., and Watanabe, Y. (2009) *J. Am. Chem. Soc.*, **131**, 6958–6960.
- 27 Takezawa, Y., Böckmann, P., Sugi, N., Wang, Z., Abe, S., Murakami, T., Hikage, T., Erker, G., Watanabe, Y., Kitagawa, S., and Ueno, T. (2011) *Dalton Trans.*, **40**, 2190–2195.
- 28 Maity, B., Fukumori, K., Abe, S., and Ueno, T. (2016) *Chem. Commun.*, **52**, 5463–5466.
- 29 He, X.M. and Carter, D.C. (1992) *Nature*, **358**, 209–215.
- 30 Albanese, D.C.M. and Gaggero, N. (2015) *RSC Adv.*, **5**, 10588–10598.
- 31 Trynda, L. and Pruchnik, F. (1995) *J. Inorg. Biochem.*, **58**, 69–77.
- 32 Bertucci, C., Botteghi, C., Giunta, D., Marchetti, M., and Paganelli, S. (2002) *Adv. Synth. Catal.*, **344**, 556–562.
- 33 Marchetti, M., Minello, F., Paganelli, S., and Piccolo, O. (2010) *Appl. Catal. A Gen.*, **373**, 76–80.
- 34 Crobu, S., Marchetti, M., and Sanna, G. (2006) *J. Inorg. Biochem.*, **100**, 1514–1520.
- 35 Kokubo, T., Sugimoto, T., Uchida, T., Tanimoto, S., and Okano, M. (1983) *J. Chem. Soc. Chem. Commun.*, 769–770.
- 36 Kohler, V., Mao, J., Heinisch, T., Pordea, A., Sardo, A., Wilson, Y.M., Knörr, L., Creus, M., Prost, J.-C., Schirmer, T., and Ward, T.R. (2011) *Angew. Chem. Int. Ed.*, **50**, 10863–10866.
- 37 Pordea, A., Creus, M., Panek, J., Duboc, C., Mathis, D., Novic, M., and Ward, T.R. (2008) *J. Am. Chem. Soc.*, **130**, 8085–8088.
- 38 Collot, J., Humbert, N., Skander, M., Klein, G., and Ward, T.R. (2004) *J. Organomet. Chem.*, **689**, 4868–4871.
- 39 van de Velde, F., Arends, I.W., and Sheldon, R.A. (2000) *Top. Catal.*, **13**, 259–265.
- 40 van de Velde, F. and Könemann, L. (1998) *Chem. Commun.*, 1891–1892.
- 41 van de Velde, Fred, Könemann, Lars, van Rantwijk, Fred, Sheldon, Roger A (2000) The rational design of semisynthetic peroxidases. *Biotechnology & Bioengineering*, **67** (1), 87–96.

- 42 McNae, I.W., Fishburne, K., Habtemariam, A., Hunter, T.M., Melchart, M., Wang, F., Walkinshaw, M.D., and Sadler, P.J. (2004) *Chem. Commun.*, 1786–1787.
- 43 Abe, S., Ueno, T., and Watanabe, Y. (2009) *Top. Organomet. Chem.*, **25**, 25–43.
- 44 Podtetenieff, J., Taglieber, A., Bill, E., Reijerse, E.J., and Reetz, M.T. (2010) *Angew. Chem. Int. Ed.*, **49**, 5151–5155.
- 45 Der, B.S., Edwards, D.R., and Kuhlman, B. (2012) *Biochemistry*, **51**, 3933–3940.
- 46 Wang, N., Zhao, X., and Lu, Y. (2005) *J. Am. Chem. Soc.*, **127**, 16541–16547.
- 47 Miner, K.D., Mukherjee, A., Gao, Y.-G., Null, E.L., Petrik, I.D., Zhao, X., Yeung, N., Robinson, H., and Lu, Y. (2012) *Angew. Chem. Int. Ed.*, **51**, 5589–5592.
- 48 Yu, Y., Cui, C., Liu, X., Petrik, I.D., and Wang, J. (2015) *J. Am. Chem. Soc.*, **137**, 11570–11573.
- 49 Zanghellini, A., Jiang, L., Wollacott, A.M., Cheng, G., Meiler, J., Althoff, E.A., Rothlisberger, D., and Baker, D. (2006) *Protein Sci.*, **15**, 2785–2794.
- 50 Kuhlman, B. and Baker, D. (2000) *Proc. Natl. Acad. Sci. U.S.A.*, **97**, 10383–10388.
- 51 Mills, J.H., Khare, S.D., Bolduc, J.M., Forouhar, F., Mulligan, V.K., Lew, S., Seetharaman, J., Tong, L., Stoddard, B.L., and Baker, D. (2013) *J. Am. Chem. Soc.*, **135**, 13393–13399.
- 52 Magis, C., Gasparini, D., Lecoq, A., Le Du, M.H., Stura, E., Charbonnier, J.B., Mourier, G., Boulain, J.C., Pardo, L., Caruana, A., Joly, A., Lefranc, M., Masella, M., Menez, A., and Cuniassé, P. (2006) *J. Am. Chem. Soc.*, **128**, 16190–16205.
- 53 Debret, G., Martel, A., and Cuniassé, P. (2009) *Nucleic Acids Res.*, **37**, W459–W464.
- 54 Zhou, L., Bosscher, M., Zhang, C., Özçubukçu, S., Zhang, L., Zhang, W., Li, C.J., Liu, J., Jensen, M.P., Lai, L., and He, C. (2014) *Nat. Chem.*, **6**, 236–241.
- 55 González, G., Hannigan, B., and DeGrado, W.F. (2014) *PLoS Comput. Biol.*, **10**, e1003750–e1003758.
- 56 Fujieda, N., Schätti, J., Stutfeld, E., Ohkubo, K., Maier, T., Fukuzumi, S., and Ward, T.R. (2015) *Chem. Sci.*, **6**, 4060–4065.
- 57 Reig, A.J., Pires, M.M., Snyder, R.A., Wu, Y., Jo, H., Kulp, D.W., Butch, S.E., Calhoun, J.R., Szyperski, T., Solomon, E.I., and DeGrado, W.F. (2012) *Nat. Chem.*, **4**, 900–906.
- 58 Faiella, M., Andreozzi, C., de Rosales, R.T.M., Pavone, V., Maglio, O., Nastri, F., DeGrado, W.F., and Lombardi, A. (2009) *Nat. Chem. Biol.*, **5**, 882–884.
- 59 Lombardi, A., Summa, C.M., Geremia, S., Randaccio, L., Pavone, V., and DeGrado, W.F. (2000) *Proc. Natl. Acad. Sci. U.S.A.*, **97**, 6298–6305.
- 60 Ulas, G., Lemmin, T., Wu, Y., Gassner, G.T., and DeGrado, W.F. (2016) *Nat. Chem.*, **8**, 354–359.
- 61 Cangelosi, V.M., Deb, A., Penner-Hahn, J.E., and Pecoraro, V.L. (2014) *Angew. Chem. Int. Ed.*, **53**, 7900–7903.
- 62 Zastrow, M.L., Peacock, A.F.A., Stuckey, J.A., and Pecoraro, V.L. (2012) *Nat. Chem.*, **4**, 118–123.

- 63 Lewis, J.C. (2015) *Curr. Opin. Chem. Biol.*, **25**, 27–35.
- 64 Hu, C., Chan, S.I., Sawyer, E.B., Yu, Y., and Wang, J. (2014) *Chem. Soc. Rev.*, **43**, 6498–6510.
- 65 Lang, K. and Chin, J.W. (2014) *Chem. Rev.*, **114**, 4764–4806.
- 66 Muir, T.W., Sondhi, D., and Cole, P.A. (1998) *Proc. Natl. Acad. Sci. U.S.A.*, **95**, 6705–6710.
- 67 Berry, S.M., Gieselman, M.D., Nilges, M.J., van der Donk, W.A., and Lu, Y. (2002) *J. Am. Chem. Soc.*, **124**, 2084–2085.
- 68 Berry, S.M., Ralle, M., Low, D.W., Blackburn, N.J., and Lu, Y. (2003) *J. Am. Chem. Soc.*, **125**, 8760–8768.
- 69 Xie, J. and Schultz, P.G. (2005) *Methods*, **36**, 227–238.
- 70 Xie, J., Liu, W., and Schultz, P.G. (2007) *Angew. Chem. Int. Ed.*, **46**, 9239–9242.
- 71 Lee, H.S. and Schultz, P.G. (2008) *J. Am. Chem. Soc.*, **130**, 13194–13195.
- 72 Bos, J., García-Herrera, A., and Roelfes, G. (2013) *Chem. Sci.*, **4**, 3578.
- 73 Drienovská, I., Rioz-Martínez, A., Draksharapu, A., and Roelfes, G. (2015) *Chem. Sci.*, **6**, 770–776.
- 74 Liu, X., Yu, Y., Hu, C., Zhang, W., Lu, Y., and Wang, J. (2012) *Angew. Chem. Int. Ed.*, **51**, 4312–4316.
- 75 Yu, Y., Zhou, Q., Wang, L., Liu, X., Zhang, W., Hu, M., Dong, J., Li, J., Lv, X., Ouyang, H., Li, H., Gao, F., Gong, W., Lu, Y., and Wang, J. (2015) *Chem. Sci.*, **6**, 3881–3885.
- 76 Zhou, Q., Hu, M., Zhang, W., Jiang, L., Perrett, S., Zhou, J., and Wang, J. (2013) *Angew. Chem. Int. Ed.*, **52**, 1203–1207.
- 77 Okeley, N.M. and van der Donk, W.A. (2000) *Chem. Biol.*, **7**, R159–R171.
- 78 Satake, Y., Abe, S., Okazaki, S., Ban, N., Hikage, T., Ueno, T., Nakajima, H., Suzuki, A., Yamane, T., Nishiyama, H., and Watanabe, Y. (2007) *Organometallics*, **26**, 4904–4908.
- 79 Kawakami, N., Shoji, O., Watanabe, Y. (2012) *Chem. bio. chem.*, **13** (14), 2045–2047.
- 80 Lelyveld, V.S., Brustad, E., Arnold, F.H., and Jasanoff, A. (2011) *J. Am. Chem. Soc.*, **133**, 649–651.
- 81 Woodward, J., Martin, N., and Marletta, M. (2006) *Nat. Methods*, **4**, 43–45.
- 82 Ozaki, S.-I., Yang, H.-J., Matsui, T., Goto, Y., and Watanabe, Y. (1999) *Tetrahedron Asym.*, **10**, 183–192.
- 83 Ozaki, S., Matsui, T., Roach, M., and Wantanabe, Y. (2000) *Coord. Chem. Rev.*, **198**, 39–59.
- 84 Fruk, L., Kuo, C.-H., Torres, E., and Niemeyer, C.M. (2009) *Angew. Chem. Int. Ed.*, **48**, 1550–1574.
- 85 Ohashi, M., Ohashi, M., Koshiyama, T., Koshiyama, T., Ueno, T., Ueno, T., Yanase, M., Yanase, M., Fujii, H., Fujii, H., Watanabe, Y., and Wantanabe, Y. (2003) *Angew. Chem. Int. Ed.*, **42**, 1005–1008.
- 86 Ueno, T., Ohashi, M., Kono, M., Kondo, K., Suzuki, A., Yamane, T., and Watanabe, Y. (2004) *Inorg. Chem.*, **43**, 2852–2858.
- 87 Ueno, T., Koshiyama, T., Ohashi, M., Kondo, K., Kono, M., Suzuki, A., Yamane, T., and Wantanabe, Y. (2005) *J. Am. Chem. Soc.*, **127**, 6556–6562.

- 88 Key, H.M., Dydio, P., Clark, D.S., and Hartwig, J.F. (2016) *Nature*, **534**, 534–537.
- 89 Ueno, T., Yokoi, N., Unno, M., Matsui, T., Tokita, Y., Yamada, M., Ikeda-Saito, M., Nakajima, H., and Watanabe, Y. (2006) *Proc. Natl. Acad. Sci. U.S.A.*, **103**, 9416–9421.
- 90 Yokoi, N., Ueno, T., Unno, M., Matsui, T., Ikeda-Saito, M., and Watanabe, Y. (2007) *Chem. Commun.*, 229–231.
- 91 Ortega-Carrasco, E., Lledos, A., and Marechal, J.D. (2014) *J. R. Soc. Interface*, **11**, 20140090.
- 92 Komatsu, T., Ishihara, S., Tsuchida, E., Nishide, H., Morokuma, C., and Nakamura, S. (2005) *Biomacromolecules*, **6**, 1489–1494.
- 93 Ricoux, R., Dubuc, R., Dupont, C., Maréchal, J.-D., Martin, A., Sellier, M., and Mahy, J.-P. (2008) *Bioconjugate Chem.*, **19**, 899–910.
- 94 Ricoux, R., Allard, M., Dubuc, R., Dupont, C., Maréchal, J.-D., and Mahy, J.-P. (2009) *Org. Biomol. Chem.*, **7**, 3208–3211.
- 95 Allard, M., Dupont, C., Muñoz Robles, V., Doucet, N., Lledos, A., Maréchal, J.-D., Urvoas, A., Mahy, J.-P., and Ricoux, R. (2011) *ChemBioChem*, **13**, 240–251.
- 96 Sagawa, T., Ishida, H., Urabe, K., and Ohkubo, K. (1991) *Chem. Lett.*, **20**, 2083–2086.
- 97 Mahammed, A., Gray, H.B., Weaver, J.J., Sorasaene, K., and Gross, Z. (2004) *Bioconjugate Chem.*, **15**, 738–746.
- 98 Mahammed, A. and Gross, Z. (2005) *J. Am. Chem. Soc.*, **127**, 2883–2887.
- 99 Zunszain, P.A., Ghuman, J., Komatsu, T., Tsuchida, E., and Curry, S. (2003) *BMC Struct. Biol.*, **3**, 6.
- 100 Watanabe, K., Ishikawa, N., and Komatsu, T. (2012) *Chem. Asian J.*, **7**, 2534–2537.
- 101 Kato, R., Kobayashi, Y., Akiyama, M., and Komatsu, T. (2013) *Dalton Trans.*, **42**, 15889–15892.
- 102 Rousselot-Pailley, P., Bochot, C., Marchi-Delapierre, C., Jorge-Robin, A., Martin, L., Fontecilla-Camps, J.C., Cavazza, C., and Ménage, S. (2009) *ChemBioChem*, **10**, 545–552.
- 103 Oliveri, V. and Vecchio, G. (2011) *Eur. J. Med. Chem.*, **46**, 961–965.
- 104 Tang, J., Huang, F., Wei, Y., Bian, H., Zhang, W., and Liang, H. (2016) *Dalton Trans.*, **45**, 8061–8072.
- 105 Reetz, M.T. and Jiao, N. (2006) *Angew. Chem. Int. Ed.*, **45**, 2416–2419.
- 106 Bos, J., Browne, W.R., Driessen, A.J.M., and Roelfes, G. (2015) *J. Am. Chem. Soc.*, **137**, 9796–9799.
- 107 Cherrier, M.V., Martin, L., Cavazza, C., Jacquamet, L., Lemaire, D., Gaillard, J., and Fontecilla-Camps, J.C. (2005) *J. Am. Chem. Soc.*, **127**, 10075–10082.
- 108 Brausam, A. and van Eldik, R. (2004) *Inorg. Chem.*, **43**, 5351–5359.
- 109 Cavazza, C., Bochot, C., Rousselot-Pailley, P., Carpentier, P., Cherrier, M.V., Martin, L., Marchi-Delapierre, C., Fontecilla-Camps, J.C., and Ménage, S. (2010) *Nat. Chem.*, **2**, 1069–1076.
- 110 Esmieu, C., Cherrier, M.V., Amara, P., Girgenti, E., Marchi-Delapierre, C., Oddon, F., Iannello, M., Jorge-Robin, A., Cavazza, C., and Ménage, S. (2013) *Angew. Chem. Int. Ed.*, **52**, 3922–3925.

- 111 Roberts, V.A., Iverson, B.L., and Iverson, S.A. (1990) *Proc. Natl. Acad. Sci. U.S.A.*, **87**, 6654–6658.
- 112 Iverson, B.L., Iverson, S.A., Roberts, V.A., Getzoff, E.D., Tainer, J.A., Benkovic, S.J., and Lerner, R.A. (1990) *Science*, **249**, 659–662.
- 113 Shokat, K.M., Leumann, C.J., Sugawara, R., and Schultz, P.G. (1988) *Angew. Chem. Int. Ed.*, **27**, 1172–1174.
- 114 Ishikawa, F., Tsumuraya, T., and Fujii, I. (2009) *J. Am. Chem. Soc.*, **131**, 456–457.
- 115 Mahy, J.P., Marechal, J.D., and Ricoux, R. (2015) *Chem. Commun.*, **51**, 2476–2494.
- 116 Reardan, D.T., Meares, C.F., Goodwin, D.A., McTigue, M., David, G.S., Stone, M.R., Leung, J.P., Bartholomew, R.M., and Frincke, J.M. (1985) *Nature*, **316**, 265–268.
- 117 Iverson, B.L. and Lerner, R.A. (1989) *Science*, **243**, 1184–1188.
- 118 Cochran, A.G. and Schultz, P.G. (1990) *Science*, **249**, 781–783.
- 119 Cochran, A.G. and Schultz, P.G. (1990) *J. Am. Chem. Soc.*, **112**, 9414–9415.
- 120 Quilez, R., de Lauzon, S., Desfosses, B., Mansuy, D., and Mahy, J.P. (1996) *FEBS Lett.*, **395**, 73–76.
- 121 Muñoz Robles, V., Maréchal, J.-D., Bahloul, A., Sari, M.-A., Mahy, J.-P., and Golinelli-Pimpaneau, B. (2012) *PLoS One*, **7**, e51128.
- 122 Ricoux, R., Lukowska, E., Pezzotti, F., and Mahy, J.-P. (2004) *Eur. J. Biochem.*, **271**, 1277–1283.
- 123 Yin, J., Mills, J.H., and Schultz, P.G. (2004) *J. Am. Chem. Soc.*, **126**, 3006–3007.
- 124 Wilson, M.E. and Whitesides, G.M. (1978) *J. Am. Chem. Soc.*, **100**, 306–307.
- 125 Lin, C.-C., Lin, C.-W., and Chan, A.S. (1999) *Tetrahedron: Asymmetry*, **10**, 1887–1893.
- 126 Ward, T.R. (2011) *Acc. Chem. Res.*, **44**, 47–57.
- 127 Kajetanowicz, A., Chatterjee, A., Reuter, R., and Ward, T.R. (2013) *Catal. Lett.*, **144**, 373–379.
- 128 Chatterjee, A., Mallin, H., Klehr, J., Vallapurackal, J., Finke, A.D., Vera, L., Marsh, M., and Ward, T.R. (2015) *Chem. Sci.*, **7**, 673–677.
- 129 Creus, M. and Ward, T.R. (2007) *Org. Biomol. Chem.*, **5**, 1835–1844.
- 130 Muñoz Robles, V., Vidossich, P., Lledos, A., Ward, T.R., and Maréchal, J.-D. (2014) *ACS Catal.*, **4**, 833–842.
- 131 Robles, V.M., Dürrenberger, M., Heinisch, T., Lledos, A., Schirmer, T., Ward, T.R., and Maréchal, J.-D. (2014) *J. Am. Chem. Soc.*, **136**, 15676–15683.
- 132 Loosli, A., Rusbandi, U.E., Gradinaru, J., Bernauer, K., Schlaepfer, C.W., Meyer, M., Mazurek, S., Novic, M., and Ward, T.R. (2006) *Inorg. Chem.*, **45**, 660–668.
- 133 Zimbron, J.M., Heinisch, T., Schmid, M., Hamels, D., Nogueira, E.S., Schirmer, T., and Ward, T.R. (2013) *J. Am. Chem. Soc.*, **135**, 5384–5388.
- 134 Hyster, T.K., Knörr, L., Ward, T.R., and Rovis, T. (2012) *Science*, **338**, 500–503.
- 135 Hyster, T.K. and Ward, T.R. (2016) *Angew. Chem. Int. Ed.*, **55**, 7344–7357.

- 136 Köhler, V., Wilson, Y.M., Dürrenberger, M., Ghislieri, D., Churakova, E., Quinto, T., Knörr, L., Häussinger, D., Hollmann, F., Turner, N.J., and Ward, T.R. (2012) *Nat. Chem.*, **5**, 93–99.
- 137 Raffy, Q., Ricoux, R., Sansiaume, E., Pethe, S., and Mahy, J.-P. (2010) *J. Mol. Cat. A Chem.*, **317**, 19–26.
- 138 Raffy, Q., Ricoux, R., and Mahy, J.-P. (2008) *Tetrahedron Lett.*, **49**, 1865–1869.
- 139 Sansiaume, E., Ricoux, R., Gori, D., and Mahy, J.-P. (2010) *Tetrahedron: Asymmetry*, **21**, 1593–1600.
- 140 Ghattas, W., Cotchico-Alonso, L., Maréchal, J.-D., Urvoas, A., Rousseau, M., Mahy, J.-P., and Ricoux, R. (2016) *ChemBioChem*, **17**, 433–440.
- 141 Sansiaume-Dagousset, E., Urvoas, A., Chelly, K., Ghattas, W., Maréchal, J.-D., Mahy, J.-P., and Ricoux, R. (2014) *Dalton Trans.*, **43**, 8344–8354.
- 142 Urvoas, A., Ghattas, W., Maréchal, J.-D., Avenier, F., Bellande, F., Mao, W., Ricoux, R., and Mahy, J.-P. (2014) *Bioorgan. Med. Chem.*, **22**, 5678–5686.
- 143 Rondot, L., Girgenti, E., Oddon, F., Marchi-Delapierre, C., Jorge-Robin, A., and Ménage, S. (2016) *J. Mol. Cat. A Chem.*, **416**, 20–28.
- 144 Kuo, C.-H., Niemeyer, C.M., and Fruk, L. (2011) *Croat. Chem. Acta*, **84**, 269–275.
- 145 Buron, C., Sénéchal-David, K., Ricoux, R., Le Caër, J.-P., Guérineau, V., Méjanelle, P., Guillot, R., Herrero, C., Mahy, J.-P., and Banse, F. (2015) *Chem. Eur. J.*, **21**, 12188–12193.
- 146 Zhao, J., Kajetanowicz, A., and Ward, T.R. (2015) *Org. Biomol. Chem.*, **13**, 5652–5655.
- 147 Monnard, F.W., Heinisch, T., Nogueira, E.S., Schirmer, T., and Ward, T.R. (2011) *Chem. Commun.*, **47**, 8238–8240.
- 148 Monnard, F.W., Nogueira, E.S., Heinisch, T., Schirmer, T., and Ward, T.R. (2013) *Chem. Sci.*, **4**, 3269–3274.
- 149 Heinisch, T., Pellizzoni, M., Dürrenberger, M., Tinberg, C.E., Kohler, V., Klehr, J., Häussinger, D., Baker, D., and Ward, T.R. (2015) *J. Am. Chem. Soc.*, **137**, 10414–10419.
- 150 Qi, D., Tann, C., Haring, D., and Distefano, M. (2001) *Chem. Rev.*, **101**, 3081–3111.
- 151 Sigman, D.S., Bruice, T.W., Mazumder, A., and Sutton, C.L. (1993) *Acc. Chem. Res.*, **26**, 98–104.
- 152 Hermanson, G.T. (1996) *Bioconjugate Techniques*, Academic Press, San Diego, CA, USA.
- 153 Reetz, M.T., Rentzsch, M., Pletsch, A., Taglieber, A., Hollmann, F., Mondiere, R.J.G., Dickmann, N., Hoecker, B., Cerrone, S., Haeger, M.C., and Sterner, R. (2008) *ChemBioChem*, **9**, 552–564.
- 154 Sletten, E.M. and Bertozzi, C.R. (2009) *Angew. Chem. Int. Ed.*, **48**, 6974–6998.
- 155 Kaiser, E.T. and Lawrence, D.S. (1984) *Science*, **226**, 505–511.
- 156 Levine, H.L., Nakagawa, Y., and Kaiser, E.T. (1977) *Biochem. Biophys. Res. Commun.*, **76**, 64–70.
- 157 Reetz, M.T., Rentzsch, M., Pletsch, A., and Maywald, M. (2002) *CHIMIA*, **56**, 721–723.

- 158 Reiner, T., Jantke, D., Marziale, A.N., Raba, A., and Eppinger, J. (2013) *ChemistryOpen*, **2**, 50–54.
- 159 Kruithof, C.A., Dijkstra, H.P., Lutz, M., Spek, A.L., Egmond, M.R., Gebbink, R.J.M.K., and van Koten, G. (2008) *Eur. J. Inorg. Chem.*, **2008**, 4425–4432.
- 160 Rutten, L., Wieczorek, B., Mannie, J.-P.B.A., Kruithof, C.A., Dijkstra, H.P., Egmond, M.R., Lutz, M., Gebbink, R.J.M.K., Gros, P., and van Koten, G. (2009) *Chem. Eur. J.*, **15**, 4270–4280.
- 161 Matsuo, T., Imai, C., Yoshida, T., Saito, T., Hayashi, T., and Hirota, S. (2012) *Chem. Commun.*, **48**, 1662–1664.
- 162 Panella, L., Broos, J., Jin, J., Fraaije, M.W., Janssen, D.B., Jeronimus-Stratingh, M., Feringa, B.L., Minnaard, A.J., and de Vries, J.G. (2005) *Chem. Commun.*, 5656–5658.
- 163 Talbi, B., Haquette, P., Martel, A., de Montigny, F., Fosse, C., Cordier, S., Roisnel, T., Jaouen, G., and Salmain, M. (2010) *Dalton Trans.*, **39**, 5605–5607.
- 164 Haquette, P., Talbi, B., Barilleau, L., Madern, N., Fosse, C., and Salmain, M. (2011) *Org. Biomol. Chem.*, **9**, 5720–5727.
- 165 Madern, N., Talbi, B., and Salmain, M. (2012) *Appl. Organomet. Chem.*, **27**, 6–12.
- 166 Basauri-Molina, M., Verhoeven, D.G.A., van Schaik, A.J., Kleijn, H., and Klein Gebbink, R.J.M. (2015) *Chem. Eur. J.*, **21**, 15676–15685.
- 167 Basauri-Molina, M., Riemersma, C.F., Würdemann, M.A., Kleijn, H., and Klein Gebbink, R.J.M. (2015) *Chem. Commun.*, **51**, 6792–6795.
- 168 Filice, M., Romero, O., Aires, A., Guisan, J.M., Rumbero, A., and Palomo, J.M. (2015) *Adv. Synth. Catal.*, **357**, 2687–2696.
- 169 Chen, C.-H.B. and Sigman, D.S. (1987) *Science*, **237**, 1197–1201.
- 170 Davies, R.R. and Distefano, M.D. (1997) *J. Am. Chem. Soc.*, **119**, 11643–11652.
- 171 Mayer, C., Gillingham, D.G., Ward, T.R., and Hilvert, D. (2011) *Chem. Commun.*, **47**, 12068–12070.
- 172 Bos, J., Fusetti, F., Driessen, A.J.M., and Roelfes, G. (2012) *Angew. Chem. Int. Ed.*, **51**, 7472–7475.
- 173 Bruice, T.W., Wise, J.G., and Rosser, D. (1991) *J. Am. Chem. Soc.*, **113**, 5446–5447.
- 174 Rana, T.M. and Meares, C.F. (1990) *J. Am. Chem. Soc.*, **112**, 2457–2458.
- 175 Greiner, D.P., Miyake, R., Moran, J.K., and Jones, A.D. (1997) *Bioconjugate Chem.*, **8**, 44–48.
- 176 Carey, J., Ma, S., Pfister, T., Garner, D., Kim, H., Abramite, J., Wang, Z., Guo, Z., and Lu, Y. (2004) *J. Am. Chem. Soc.*, **126**, 10812–10813.
- 177 Platis, I.E., Ermácora, M.R., and Fox, R.O. (1993) *Biochemistry*, **32**, 12761–12767.
- 178 Erlanson, D.A., Chytil, M., and Verdine, G.L. (1996) *Chem. Biol.*, **3**, 981–991.
- 179 Laan, W., Muñoz, B.K., den Heeten, R., and Kamer, P.C.J. (2010) *ChemBioChem*, **11**, 1236–1239.
- 180 Deuss, P.J., Popa, G., Botting, C.H., Laan, W., and Kamer, P.C.J. (2010) *Angew. Chem. Int. Ed.*, **49**, 5315–5317.

- 181 Traviglia, S.L., Datwyler, S.A., and Meares, C.F. (1999) *Biochemistry*, **38**, 4259–4265.
- 182 Ishihama, A. (2000) *Chem. Commun.*, 1091–1094.
- 183 van Dongen, S. F. M., Clerx, J., Nørgaard, K., Bloemberg, T. G., Cornelissen, J. J. L. M., Trakselis, M. A., Nelson, S. W., Benkovic, S. J., Rowan, A. E., Nolte, R. J. M. (2013) *Nat Chem*, **5** (11), 945–951.
- 184 Davies, R.R., Kuang, H., Qi, D.F., Mazhary, A., Mayaan, E., and Distefano, M.D. (1999) *Bioorg. Med. Chem. Lett.*, **9**, 79–84.
- 185 Ory, J.J., Mazhary, A., Kuang, H., Davies, R.R., Distefano, M.D., and Banaszak, L.J. (2013) *Nat. Chem.*, **5**, 945–951.
- 186 Sauer, D.F., Bocola, M., Broglia, C., Arlt, M., Zhu, L.-L., Brocker, M., Schwaneberg, U., and Okuda, J. (2014) *Chem. Asian J.*, **10**, 177–182.
- 187 Rother, M., Nussbaumer, M.G., Renggli, K., and Bruns, N. (2016) *Chem. Soc. Rev.*, **45**, 6213–6249.
- 188 Onoda, A., Fukumoto, K., Arlt, M., Bocola, M., Schwaneberg, U., and Hayashi, T. (2012) *Chem. Commun.*, **48**, 9756–9758.
- 189 Onoda, A., Kihara, Y., Fukumoto, K., Sano, Y., and Hayashi, T. (2014) *ACS Catal.*, **4**, 2645–2648.
- 190 Springer, J.W., Parkes-Loach, P.S., Reddy, K.R., Krayner, M., Jiao, J., Lee, G.M., Niedzwiedzki, D.M., Harris, M.A., Kirmaier, C., Bocian, D.F., Lindsey, J.S., Holten, D., and Loach, P.A. (2012) *J. Am. Chem. Soc.*, **134**, 4589–4599.
- 191 Harris, M.A., Parkes-Loach, P.S., Springer, J.W., Jiang, J., Martin, E.C., Qian, P., Jiao, J., Niedzwiedzki, D.M., Kirmaier, C., Olsen, J.D., Bocian, D.F., Holten, D., Hunter, C.N., Lindsey, J.S., and Loach, P.A. (2013) *Chem. Sci.*, **4**, 3924–3933.
- 192 Wilson, Y.M., Dürrenberger, M., Nogueira, E.S., and Ward, T.R. (2014) *J. Am. Chem. Soc.*, **136**, 8928–8932.
- 193 Gu, Y., Ellis-Guardiola, K., Srivastava, P., and Lewis, J.C. (2015) *Chem-BioChem*, **16**, 1880–1883.
- 194 Romero, P.A. and Arnold, F.H. (2009) *Nat. Rev. Mol. Cell Biol.*, **10**, 866–876.
- 195 Muñoz Robles, V., Ortega-Carrasco, E., Alonso-Cotchico, L., Rodriguez-Guerra, J., Lledos, A., and Maréchal, J.-D. (2015) *ACS Catal.*, **5**, 2469–2480.